

Annual Review of Materials Research

Extreme Abnormal Grain Growth: Connecting Mechanisms to Microstructural Outcomes

Carl E. Krill III,¹ Elizabeth A. Holm,² Jules M. Dake,¹ Ryan Cohn,³ Karolína Holíková,¹ and Fabian Andorfer¹

¹Institute of Functional Nanosystems, Ulm University, Ulm, Germany; email: carl.krill@uni-ulm.de, jules.dake@uni-ulm.de, karolina.holikova@uni-ulm.de, fabian.andorfer@uni-ulm.de

Annu. Rev. Mater. Res. 2023. 53:15.1-15.27

The *Annual Review of Materials Research* is online at matsci.annualreviews.org

https://doi.org/10.1146/annurev-matsci-080921-091647

Copyright © 2023 by the author(s). All rights reserved

Keywords

abnormal grain growth, grain boundary energy, grain boundary mobility, grain growth-induced microstructure, Zener pinning

Abstract

If variety is the spice of life, then abnormal grain growth (AGG) may be the materials processing equivalent of sriracha sauce. Abnormally growing grains can be prismatic, dendritic, or practically any shape in between. When they grow at least an order of magnitude larger than their neighbors in the matrix—a state we call extreme AGG—we can examine the abnormal/matrix interface for clues to the underlying mechanism. Simulating AGG for various formulations of the grain boundary (GB) equation of motion, we show that anisotropies in GB mobility and energy leave a characteristic fingerprint in the abnormal/matrix boundary. Except in the case of prismatic growth, the morphological signature of most reported instances of AGG is consistent with a certain degree of GB mobility variability. Open questions remain, however, concerning the mechanism by which the corresponding growth advantage is established and maintained as the GBs of abnormal grains advance through the matrix.



²Department of Materials Science and Engineering, University of Michigan, Ann Arbor, Michigan, USA; email: eaholm@umich.edu

³Department of Materials Science and Engineering, Carnegie Mellon University, Pittsburgh, Pennsylvania, USA; email: rcohn@cmu.edu

1. INTRODUCTION

1.1. Defining Abnormal Grain Growth

Abnormal grain growth (AGG) is surprisingly difficult to define. AGG occurs when a few grains in a polycrystalline material grow at the expense of all the others. This alone does not distinguish AGG from normal grain growth (NGG), however, since during NGG it is also the case that some grains grow while others shrink. A differentiating feature of AGG is the disproportionate growth of a certain fraction of grains—the abnormal component—to the point that a bimodal grain size distribution (GSD) develops and persists over time (1-3). But even this distinction is not unambiguous: When only a few abnormal grains are present or their size advantage is small, the abnormal grain peak in the GSD may be dwarfed by the normal peak such that AGG may not be statistically apparent.

On the other hand, AGG can sometimes be microstructurally obvious, as in the examples shown in Figure 1. Even though the abnormally large grains visible in these micrographs take on a variety of sizes and morphologies, their anomalous nature is unmistakable. In this review, we focus on instances of what we shall call extreme AGG, which occurs when the abnormal grains attain and maintain a size that is at least an order of magnitude larger than that of the normal grains in the polycrystal. If, at a given time t, we group all abnormally growing grains (a) into a set of grain sizes $\{R_a(t)\}\$ and the remaining grains—the matrix (m)—into the complementary set $\{R_m(t)\}\$, then we identify the occurrence of extreme AGG by fulfillment of the condition $\langle R_a(t) \rangle > 10 \langle R_m(t) \rangle$, whereby $\langle \cdot \rangle$ denotes an appropriate average (3). By focusing on such obvious cases of AGG, we sidestep the challenging task of distinguishing weak manifestations of abnormality (in particular, during incipient stages of AGG) from transient periods of NGG (4). Even more importantly, we anticipate that measurable ramifications of the mechanisms underlying AGG will be most pronounced at the extreme limit, which should facilitate relating characteristics of the resulting microstructure to physical processes. Note that the phenomenological signature of extreme AGG may be lost if the subpopulation of abnormally growing grains manages to consume nearly all of the matrix, since, once this point has been reached, the GSD will likely have reverted to a unimodal shape.

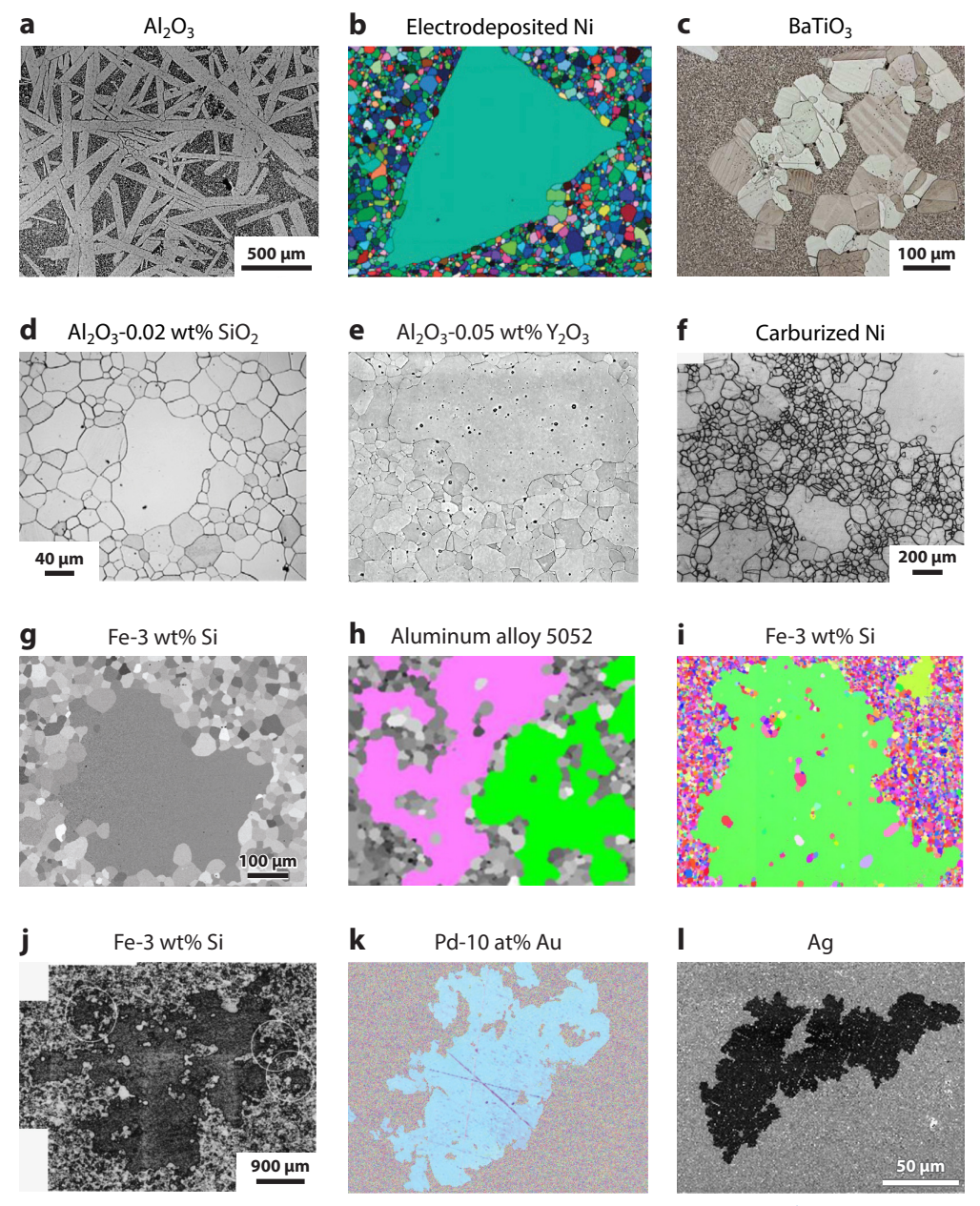
As Figure 1 illustrates, few phenomena associated with materials processing rival the sheer morphological diversity induced by AGG, with abnormally growing grains sometimes emerging from a sea of smaller grains in the form of large, faceted structures, such as plates or cubes (Figure 1a-c) (5-7); roughly equiaxed regions bounded by gently curved faces, rather like highly magnified versions of the smaller neighboring grains (Figure 1d-f) (8–10); or—perhaps most strikingly-dendritic structures, the shapes of which suggest tentacular penetration by an abnormal grain into its surroundings, reminiscent of the manner in which a tumor cell invades nearby tissue (Figure 1g-l) (11-16). Despite the marked differences in abnormal grain morphology in each case, the telltale sign of AGG is the much faster coarsening of the abnormal component relative to the remaining grains in the polycrystal.

The wide variety of AGG microstructures has led to a corresponding diversity in terminology for what is essentially the same phenomenon. Cyril Stanley Smith referred to "runaway grains" (17, pp. 152-53), although this nomenclature was not widely adopted. AGG has also been called "secondary grain growth" (18), "discontinuous grain growth" (19-22), or "secondary recrystallization" (3, 23, 24). Complicating matters, some of these terms are used when discussing only a particular subset of AGG phenomena, sometimes in contradictory ways. For example, secondary recrystallization can refer to surface energy-driven AGG (23), especially in the context of electronic materials, or to AGG governed by grain boundary (GB) properties (24), particularly when it occurs in transformer steels. Of course, as pointed out by Raabe (3), secondary recrystallization



does not denote a form of recrystallization but rather one of grain growth. Here, we employ the term AGG to encompass the entire gamut of abnormal growth processes, and we treat the different flavors as subtypes of the overall phenomenon.

It should be noted that various aspects of recrystallization can resemble characteristics of extreme AGG. In fact, recrystallization can be considered to be a type of AGG that is driven by the removal of stored strain energy (dislocations). Because recrystallization is studied as a distinct and



(Caption appears on following page)



Figure 1 (Figure appears on preceding page)

Experimental examples of extreme abnormal grain growth, as observed in a variety of materials. In the first row (a-c), the abnormal grains appear to grow as if decoupled from the matrix. The abnormal grains of the second row (d-f) take on comparatively more circular and compact shapes, almost as if they represent highly magnified versions of the matrix grains. The abnormal grains visible in the remaining micrographs (g-l) manifest quite irregular morphologies. At their outer edges, the abnormal grains have tentacle-like protrusions that extend into the matrix; moreover, the grain interiors are marked by island grains that appear to have been cut off or orphaned by the rapid expansion of the abnormal grain. Panels d-l are arranged in order of decreasing circularity of the abnormal grain (see Section 3.2). Panels a, c, d, i, and l adapted from References 5, 7, 8, 13, and 16, respectively, with permission from Elsevier. Panel b adapted from Reference 6 with permission from Taylor & Francis. Panel e adapted with permission from Reference 9; copyright 2003 American Ceramic Society. Panels f and b adapted from References 10 and 12, respectively, with permission from Springer. Panel g adapted from Reference 11 with permission from Trans Tech Publications. Panel j adapted from Reference 14 with permission from AIP Publishing. Panel k adapted from Reference 15 with permission from the authors.

> well-defined phenomenon—one that has been extensively reviewed elsewhere (2, 3)—we neither classify it as AGG nor include it in this review, except where needed to contrast with AGG.

> Finally, in this review, we focus on AGG in bulk materials, which is driven by the elimination of excess energy stored in GBs. This covers a broad range of AGG scenarios, but it necessarily excludes some important cases. For example, AGG in textured thin films is often driven by the reduction in surface energy. This mode of AGG is widely observed and well understood (18, 25–27), so we do not treat it here. Likewise, AGG may be driven by volumetric driving forces, such as strain fields (28), stress fields (21), phase transformations (29), or magnetic coupling (30). Since these cases proceed more analogously to phase transformations, they are not addressed in this review.

1.2. Technological Implications of Abnormal Grain Growth

Predicting if and when AGG will occur in a given system has long been a holy grail of materials processing. The technological motivation behind resolving this issue stems from the largely deleterious properties associated with bimodality of the GSD. In ductile materials, the Hall-Petch relation (31) indicates that larger grains tend to be mechanically softer than smaller counterparts of the same composition, which means that, when subjected to an applied load, the interfaces between abnormal and matrix grains are likely to deform inhomogeneously, leading to the formation of internal cracks (32). In brittle materials, large grains may be critical flaws from the point of view of fracture toughness (33). Even under conditions of low loading, the mere presence of a few large grains embedded in a much finer matrix can have negative consequences, such as the roping discovered in certain Al alloys considered by automobile manufacturers for possible use in body panels (34). Rolling elongates the abnormal grains, which then recrystallize into bands of finer grains sharing a similar orientation. The resulting inhomogeneity is readily noticeable in the form of paint-brush lines (35), which are contours visible even after the panel surfaces have been painted.

Conversely, there are instances in which AGG is actually found to be beneficial, such as when it facilitates the growth of low-resistivity Cu interconnects (36, 37); when it leads to reduced losses in the cores of electrical transformers, the application for so-called electrical steels (38, 39); when it enhances recoverability in shape-memory alloys (40); or when it contributes to improved magnetostrictive properties (41). In ceramic materials, the abnormal growth of elongated grains has been found to increase fracture toughness by the crack-bridging mechanism (42). A highly bimodal GSD improves the ductility of bulk specimens of Cu rolled at liquid nitrogen temperature followed by a short annealing step at 200°C, which triggers recrystallization and AGG (43, 44). When cycled, such thermomechanical treatments can induce dynamic AGG (28), which has been exploited to grow ultralarge single crystals (45-47). In most of these cases, however, the pivotal role played by AGG turned out to be a fortuitous discovery rather than a feature deliberately designed into the processing route.



1.3. A Taxonomy of Microstructures Generated by Extreme Abnormal **Grain Growth**

The micrographs collected in Figure 1 attest to the wide variety of microstructures that can arise from extreme AGG. A possible classification scheme could be based on a comparison of the curvature of interfaces between abnormal and matrix grains with the curvature of interfaces between matrix grains. In cases such as those shown in Figure 1a-c, most parts of the abnormal/matrix interface are faceted or nearly flat, whereas the matrix/matrix boundaries have mean curvatures comparable to $\langle R_{\rm m} \rangle^{-1}$. The opposite limiting case is represented by the representative microstructures shown in **Figure 1***g***–***I*, for which the interfaces between abnormal and matrix grains appear to be just as convoluted locally as typical segments of the GB network in the matrix region. The intermediate case of moderately curved abnormal/matrix boundaries is also possible, as shown in Figure 1*d*–*f*.

Any mechanism that purports to capture the physics underlying a particular form of extreme AGG will necessarily have to account for the morphology of the abnormal/matrix interface—in particular, in comparison to that of matrix/matrix GBs in the same specimen. The huge variation in observed abnormal GB morphologies suggests the likely existence of more than one cause for extreme AGG. Whatever that cause may be, it is clear that an abnormal grain can emerge from the matrix only by comparatively much faster migration of the abnormal/matrix interface; logically, it follows that one or more of the properties of those particular GBs—be they structural, thermodynamic, or kinetic—must play a critical role in the occurrence of AGG. In extreme cases, it may be possible to detect the property or properties of greatest relevance to AGG simply by examining which abnormal/matrix GB characteristics diverge most severely from those of matrix/matrix GBs.

2. PHENOMENOLOGY OF ABNORMAL GRAIN GROWTH

One reason for the difficulty of predicting when grain growth will proceed abnormally versus normally can be traced to the fact that, in both cases, the microstructure of a polycrystalline specimen evolves to lower the excess free energy ΔG^{GB} stored in the network of GBs (2). (As noted above, we exclude coarsening driven primarily by strain energy—i.e., recrystallization—or by other energies stored in grain volumes rather than their boundaries.) Consequently, there is no fundamental physical difference in the driving force—more correctly, the driving pressure—acting on GBs during AGG and NGG.

The quantity $\Delta G^{\rm GB}$ can be expressed as the (average) excess energy per unit of GB area, γ , multiplied by the overall GB area, A^{GB} . If we stipulate a fixed value for γ , then the only possibility for a given GB to minimize its contribution to ΔG^{GB} would be by migrating so as to reduce its area—for instance, by flattening out curved regions or by shrinking (perhaps to the point of disappearance). Regardless of whether this process proceeds normally or abnormally, once GB migration has resulted in a grain having surrendered all of its atoms to neighboring grains, the former ceases to exist, and the specimen will have moved closer toward the single-crystalline ground state (i.e., $\Delta G^{\rm GB} = 0$).

Citing experimental evidence for the migration of a curved GB toward its center of curvature (49), Burke & Turnbull (50) postulated the existence of a curvature-based driving force for GB migration, $\gamma \cdot \kappa(\mathbf{r})$, where $\kappa(\mathbf{r})$ denotes the mean curvature at a given point \mathbf{r} on the GB. The





¹More precisely, the free energy driving force for boundary motion involves the GB stiffness (48), which includes contributions from the boundary plane normal. As noted for γ , the GB stiffness can vary with position and may entail considerable anisotropy. For the sake of consistency with established conventions in the literature on grain growth, we refer to the driving force as the product of the GB energy γ and the curvature κ , understanding that additional stiffness terms may nevertheless be relevant.

translational speed $v^{GB}(\mathbf{r})$ of this GB location is assumed to be linearly proportional to the driving force acting at that point,

$$v^{\text{GB}}(\mathbf{r}) = \mu(\mathbf{r}) \cdot \gamma(\mathbf{r}) \cdot \kappa(\mathbf{r}),$$
 1.

wherein the constant of proportionality μ is called the GB mobility, and, in general, μ and γ can each vary with the location r. Computational implementations of the simplest possible realization of Equation 1—in which both $\mu(\mathbf{r}) \equiv \mu$ and $\gamma(\mathbf{r}) \equiv \gamma$ are held constant over the entire network of GBs (sometimes called the assumption of ideal grain growth)—find that the GSD invariably evolves toward a unimodal shape, even if the starting grain configuration is highly bimodal (51). In addition, there are no signs of incipient abnormality in the growth behavior of individual grains, even when the latter happen to start out much larger than their neighbors (52, 53). In fact, under mean-field conditions for the ideal growth case, it has been proven analytically that a polycrystalline microstructure must evolve asymptotically toward the GSD dictated by NGG (25, 54).

Evidently, the emergence of AGG cannot be encoded in the equation of motion for GBs (Equation 1) solely in terms of the distribution of GB curvatures $\kappa(\mathbf{r})$, as pure curvature flow tends toward NGG. The origin of abnormality, then, must somehow be traceable to certain characteristics of $\gamma(\mathbf{r})$ and/or $\mu(\mathbf{r})$ [in addition to $\kappa(\mathbf{r})$].

2.1. Grain-Based Criteria for Abnormal Grain Growth

Before investigating the extent to which specific modifications of Equation 1 can induce AGG, we consider the general conditions for AGG that are imposed by the phenomenology of the process itself. The characteristic indicator for AGG is the faster growth of a subpopulation of grains that persists over time. Let R denote the size of a given grain and $\langle R \rangle$ the (number-weighted) average grain size. At a given time t, we say that a specific grain is growing abnormally if and only if it manifests a growth advantage as well as persistence.

2.1.1. Growth advantage. For an abnormal grain (a) growing into a region occupied by matrix grains (m), the size of the abnormal grain, R_a , must increase faster than the average matrix grain size $\langle R_{\rm m} \rangle$. For grain growth in 2D, Rollett & Mullins (54) and Rollett (55) derived the following mean-field expression for the condition:

$$\frac{\mathrm{d}\rho(t)}{\mathrm{d}t} = \frac{\mu_{\mathrm{mm}}\gamma_{\mathrm{mm}}}{2\langle R_{\mathrm{m}}\rangle^{2}} \left\{ M\Gamma \left[A + \frac{A-2}{\rho(t)} \right] - \frac{\rho(t)}{4} \right\} > 0,$$
2.

where $\rho(t)$ denotes the ratio $R_a/\langle R_m \rangle$ at time t and μ_{mm} and γ_{mm} are the mobility and energy, respectively, of GBs between two matrix grains (mm). Abnormal/matrix (am) boundaries enter Equation 2 through the ratios $M = \mu_{\rm am}/\mu_{\rm mm}$ and $\Gamma = \gamma_{\rm am}/\gamma_{\rm mm}$, and A stands for $(6/\pi)\sin^{-1}[1/(2\Gamma)]$. The sign of the right-hand side of this equation is determined by the expression in braces, whereby M>1 (the abnormal grain has higher-mobility boundaries) and $\Gamma<1$ (the abnormal grain has lower-energy boundaries) expand the range in ρ over which AGG is observed (54)—a conclusion that holds for grain growth in 3D, as well. It is worth noting that the growth advantage in Equation 2 is intrinsically time-limited; the form of the equation ensures that the growth advantage peaks at a particular time determined by M and Γ , remaining stable or decreasing thereafter (56).

2.1.2. Persistence. Even in a unimodal GSD induced by NGG, there will always be a few grains that, at any given instant, happen to be growing faster than the average grain size; in other words, they fulfill Equation 2 at a particular time t. However, if such a grain has grown significantly



larger than its neighbors, it must have maintained this growth advantage over a range of times $[t_0, t]$ sufficient to reach a grain size much greater than $\langle R_{\rm m} \rangle$. During this time interval, the abnormally growing grain consumes matrix grains in its immediate vicinity and impinges upon new neighbors. In the Rollett-Mullins model, all matrix grains are equivalent, so the evolving microstructural environment does not change the abnormal grain's growth trajectory. However, in real microstructures, any modifications of the abnormal grain's surroundings may alter its ability to persist in comparatively rapid growth.

2.2. The Nature of the Growth Advantage

A bimodal GSD—and thus AGG—can arise in a given polycrystalline microstructure only if a subpopulation of grains meets the condition outlined in Section 2.1.1 as well as the one in Section 2.1.2; that is, the abnormal component must be able to capitalize on some form of growth advantage, while simultaneously exploiting a mechanism to maintain this advantage as the microstructural environment evolves.

In order for grains to grow spontaneously, the process must be thermodynamically favored. For grain growth driven by the elimination of GB free energy, this requirement can be projected onto individual grains, resulting in the condition that a given grain will grow only if the mean boundary curvature integrated over all of its boundaries is positive (57). In practice, this is usually correlated with having a larger-than-average size. As long as its boundaries are mobile, a grain fulfilling this criterion will grow during NGG, but this does not guarantee that the grain in question will grow faster than the average grain size—that is, abnormally. To manifest the kind of growth advantage needed for AGG, the candidate grain must be thermodynamically favored to grow and have an additional energetic or kinetic advantage that enables it to grow faster than the other grains in the polycrystal.

Thus, even though a persistent gap in size between abnormal grains and their matrix counterparts is the most prominent indicator for extreme AGG, abnormally rapid growth is best understood not as a grain-based phenomenon but rather as one occurring on a polycrystal's network of interconnected GBs. In that vein, we should recast the grain-based formulations of growth advantage (Section 2.1.1) and persistence (Section 2.1.2) into expressions that depend on the properties of individual GBs. For this purpose, the Burke-Turnbull equation for curvature-driven GB migration (Equation 1) provides a helpful starting point, as its component terms are already specific to individual boundaries. In principle, the quantities appearing on the right-hand side of Equation 1—the mobility $\mu(\mathbf{r})$, energy $\gamma(\mathbf{r})$, and curvature $\kappa(\mathbf{r})$ —can vary not only from GB to GB but also from point to point on the same GB. However, since all locations on, say, the ith GB in the network must migrate together, it is common to assign average values for the mobility $\langle \mu \rangle_i$ and energy $\langle \gamma \rangle_i$ to each position \mathbf{r}_i on the same GB. (The simplifications behind ideal grain growth are even more drastic, of course, since, in that case, $\langle \mu \rangle_i \equiv \mu$ and $\langle \gamma \rangle_i \equiv \gamma$ for all *i*.)

We know from experimental measurements (1, 58-61) and atomistic simulations (62-67) that in real polycrystals both $\langle \mu \rangle_i$ and $\langle \gamma \rangle_i$ can vary strongly from GB to GB. In fact, $\langle \mu \rangle_i$ has a dynamic range covering three or more orders of magnitude (59, 60, 63), and $\langle \gamma \rangle_i$ varies over approximately a factor of 10 (1, 62). Therefore, it is relevant to consider the physical basis for growth advantages potentially conferred by $\langle \mu \rangle_i$ and $\langle \gamma \rangle_i$.



²Owing to the connectivity of the GB network, it is not necessarily the largest values of mobility or energy that have the greatest impact on grain growth, since the evolution of a local region of the GB network will generally be governed by the more slowly migrating GBs (68). Even if some of these GBs have the potential to migrate more quickly, they may be hindered from doing so by virtue of being connected to slower boundaries;

2.2.1. Growth advantage arising from variations in grain boundary energy. The GB free energy γ is a thermodynamic state variable that depends on the atomic structure of the boundary (62, 69, 70) as well as on the formation of GB complexions (8), including the adsorption of solute species at the boundary (71, 72). In addition to these intrinsic thermodynamic factors, there is the possibility for GBs to occupy nonequilibrium, higher-energy states (especially while moving) (66) or for different GB structures to be energetically degenerate (73). Note that Equation 2 suggests that lower-energy GBs (i.e., $\Gamma < 1$) are more conducive to the occurrence of AGG in a particular region of the GB network despite the proportionality of v^{GB} to γ in Equation 1—a relation that implies a decrease in γ would tend to slow down an abnormal/matrix GB.

The intrinsic, or structural, GB energy depends on the crystallographic misorientation between the two grains that share the boundary (as well as on the GB inclination and any atomic reconstruction that occurs in the interface). Most GBs of very low energy are either low-misorientation angle boundaries (69) or associated with special crystallographic relationships between the grains (74). This has an impact on the GB energy relationships that can arise in a polycrystal. For example, it is crystallographically unlikely for a grain to have low-misorientation GBs with a set of grains that all have high-misorientation GBs with respect to each other (75).³ This makes AGG by boundary wetting or triple-junction intrusion an improbable scenario.

A similar issue arises with the proposed subgrain-boundary-enhanced solid-state wetting (SB-SSW) mechanism for AGG (77, 78). In metals, it is not uncommon for grains to contain very low-angle, low-energy GBs (subgrain boundaries) that organize during recovery after deformation. In the SB-SSW model for AGG, these subgrain boundaries replace higher-energy GBs and, in so doing, facilitate growth of their parent grain. Considering the subgrain boundary as a GB, we see that It separates two grains A' and A" that have almost identical orientations (and, indeed, are just slight rotations of the parent grain A). Both A' and A" share high-angle boundaries with a third grain B. The SB-SSW process requires the low-angle boundary A'A" to replace one of the highangle boundaries, A'B or A"B. Energetically, this is favored when $\gamma(A'A'') < |\gamma(A'B) - \gamma(A''B)|$. Application of the Read-Shockley GB energy function (69) shows that this scenario is extremely unlikely.⁴ High-angle boundaries between substantially similar pairs of grains (A'B and A"B) do not differ in energy by an amount comparable to that of even a quite low-angle subgrain boundary (A'A"), so an SB-SSW occurrence would represent a rare event—not one that a given grain could persist in replicating during AGG. Although the SB-SSW mechanism is thermodynamically feasible, in real microstructures it is not a plausible mechanism for AGG and has not been widely observed experimentally (80, 81).

For some boundaries, the GB energy can be well approximated by the sum of the energies of the two abutting crystal planes (82). This is especially relevant in highly covalent materials or in systems in which a solute or liquid layer separates the two grains. If one of the grains adopts a low-energy—or even singular (i.e., atomically flat)—boundary plane, it can have an energetic advantage for growth. Because the grain will grow while preserving the low-energy plane, the abnormal grain will be strongly faceted, displaying flat faces. Growth here is not by curvature but by direct consumption of the matrix GBs, as they are swept out by the flat facets (83). The key point here is that the low-energy boundary plane must be maintained regardless of the matrix



in this case, according to Equation 1, the curvature term will adjust to correspond to the actual (lower) speed of each GB's migration.

³The reverse situation—a grain that has high-misorientation GBs with a set of grains that form low-misorientation GBs with respect to each other—can and does occur in highly textured samples (76).

⁴Triple line wetting is also possible, with somewhat less restrictive energetic constraints (79). The required crystallographic relationships remain similar, however.

grains it encounters. We refer to this scenario as decoupled AGG, and it is illustrated by the micrographs in Figure 1a-c. Among the unresolved issues plaguing our understanding of this mode of AGG are the questions of why only certain grains acquire the favored low-energy facets and what mechanism insulates the low-energy facets from their crystallographic neighborhood. It is generally supposed that impurities play an important role.

2.2.2. Growth advantage arising from variations in grain boundary mobility. According to Equation 1, the GB mobility μ is a kinetic property that scales the rate of GB migration with the driving force. In pure materials, μ depends on the defect structure of the boundary and the atomic rearrangements required to move the defects (63, 84, 85). During grain growth, boundary mobility may be influenced by interactions with bulk defects (86), irradiation (87), faceting (10), or the process of GB migration itself (84). GB defects may couple with different driving forces in diverse ways (84). Thus, even in pure materials, the GB mobility may be a complex and timevarying property. When combined with extrinsic factors, including segregating solutes (88), GB complexions (8), and GB grooving (89), there is considerable opportunity for GBs to have widely varying mobilities, as noted in another review in this volume (90). AGG is favored for grains with high-mobility boundaries.

2.2.3. Combined energetic and kinetic contributions. The pinning of GBs by second-phase particles is well known to be associated with AGG (91, 92). Both the energetics and the kinetics of GBs play a part in making this possible. When migrating GBs encounter second-phase particles, the overall interfacial energy decreases. As Smith & Zener demonstrated (93), a sufficient number of particle/boundary intersections can overcome the curvature-based driving force and pin a GB. Because the intersecting particles lower a GB's area and, consequently, its energy, a particlepinned boundary is thermodynamically held in place; it retains its intrinsic mobility, but it cannot move. If such a GB later regains the ability to migrate, it will have a mobility advantage relative to the still-pinned GBs, thereby potentially leading to AGG (92, 94). This can be precipitated by a nonuniform particle distribution (95), the dissolution of pinning particles near the solvus temperature (96, 97), or thermal fluctuations of the boundary itself (98). Essentially, the thermodynamic pinning of matrix grains provides the unpinned grain with the mobility advantage required for AGG. A similar situation can occur when solute atoms have segregated to the GBs. Although the thermodynamic (99) and kinetic (100) effects of solute segregation can hinder boundary migration,⁵ breakaway from a solute cloud can confer a mobility advantage to the unencumbered GB (102-104).

In real materials, AGG growth advantage mechanisms are often coupled, whether cooperatively (e.g., a large grain having high-mobility GBs) or competitively (e.g., high-mobility GBs having high energies). A strong point of computer simulations is their ability to isolate mechanisms to study their particular effects. The top row of images in Figure 2 shows abnormal grains generated by various persistent growth advantages, as simulated by the Monte Carlo Potts model (MCPM), with a superposed cellular automaton (CA) model in the case of decoupled AGG. (These methods are discussed in greater detail in Section 2.5.) Distinct grain morphologies develop for the different advantage mechanisms. As noted previously, a size advantage alone does not lead to AGG, and the resulting grain is large but normal. If a candidate grain is given low-energy GBs with its neighbors, it acquires a lacy, concave shape, and sharp dihedral angles form at triple junctions penetrating along matrix/matrix GBs. In contrast, a GB mobility advantage results in a scalloped, convex grain shape that tends to include peninsulas and islands comprised of matrix



⁵In rare cases, the presence of a segregant species at a GB can have the opposite effect, leading to more rapid GB migration (101).

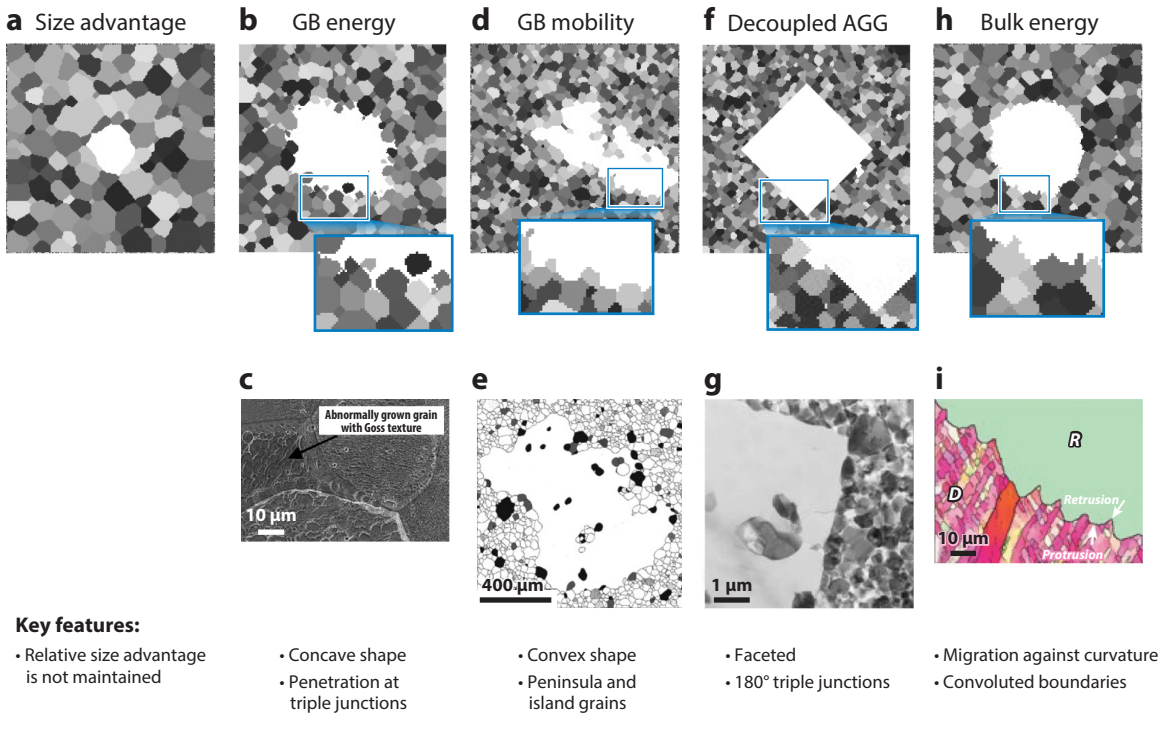


Figure 2

Abnormal grain morphologies generated by specific (persistent) growth advantages. The top row shows microstructures simulated by the Monte Carlo Potts model (with a superposed cellular automaton model in the case of decoupled AGG); the insets highlight characteristic growth features. The bottom row gives examples of similar experimental observations. Starting on the left, (a) a grain given an initial size advantage does not grow abnormally but rejoins the grain size distribution dictated by normal grain growth. (b,c) A GB energy advantage (in this case, $\Gamma = 0.5$) yields an abnormal grain with concave boundaries that penetrate along triple junctions. (d,e) In contrast, a GB mobility advantage (here, M=1,000) leads to roughly convex abnormal/matrix interfaces marked by peninsula-shaped regions and/or island grains. (f,g) Decoupled AGG is characterized by faceted boundaries and a 180° dihedral angle at triple junctions. (h,i) A bulk energy advantage (i.e., recrystallization) involves GB migration against curvature and convoluted boundary morphologies. Micrographs reproduced from (c) Reference 14 (with permission from AIP Publishing), (e) Reference 105 (copyright 2019 The Japan Institute of Metals), (g) Reference 106 (with permission from Elsevier), and (i) Reference 107 (copyright 2013 American Physical Society). Abbreviations: AGG, abnormal grain growth; GB, grain boundary; R, recrystallized grain; D, deformed grains.

> grains. When high-mobility GBs are decoupled from the matrix grains, prismatic shapes can grow. A bulk energy driving force, as encountered during recrystallization, can overcome the GB energy, yielding convoluted boundary morphologies, the fluctuation spectrum of which can extend to subgrain length scales. These characteristic features are also observed in experimental systems, with specific examples shown in the bottom row of Figure 2.

> Finally, we should note that it is not necessary for each boundary of an abnormal grain to have a persistent growth advantage in order for the grain to grow abnormally. As we discuss in Section 3.2, AGG requires only a certain fraction of an abnormal grain's boundaries to have an advantage at any given time, and the shape of the resulting grain will depend on that fraction.

2.3. Reformulating the Growth Advantage in Terms of Grain Boundary Speed

As befits a phenomenon with such diverse manifestations, many different scenarios can give rise to AGG. The growth advantage may involve energetic, kinetic, or combined contributions, not



all of which are captured in Equation 2. The common denominator, however, is a grain whose growth rate outstrips that of its competitors. Thus, assuming that the jth grain is growing abnormally at time t, we can reformulate the growth advantage criterion in terms of the average speed of the grain's abnormal/matrix interfaces, $\langle |v_{\rm am}(t)| \rangle_i$, where averaging is performed over only the boundaries of grain j, and the absolute value ensures that the migration speed is treated as an unsigned quantity. Because the speed of a moving boundary is governed by its energy, mobility, and curvature as well as by its microstructural environment, this framing incorporates thermodynamic, kinetic, and connectivity factors that affect GB motion. The grain-based criteria for AGG of Sections 2.1.1 and 2.1.2 can be recast in terms of GB migration rates:

- 1. With respect to growth advantage, the average speed of abnormally growing grain i's GBs, $\langle |v_{\rm am}(t)| \rangle_j$, must be much greater than the average migration speed of matrix/matrix GBs, $\langle |v_{\rm mm}(t)| \rangle$, at the same moment in time: $\langle |v_{\rm am}(t)| \rangle_i \gg \langle |v_{\rm mm}(t)| \rangle$.
- 2. With respect to persistence, at a given time t, AGG occurs only if a stable subpopulation of grains has fulfilled the growth advantage criterion over a time interval $[t_0, t]$ of sufficient duration to grow much larger than the matrix grains.

Note that these expressions obscure the fact that the set of abnormal/matrix GBs changes with time. Whenever an abnormally growing grain consumes one of its neighbors, any interface shared with that neighbor disappears for good from the GB network; in fact, once the entire complement of nearest-neighbor grains has fallen victim to an abnormal grain's expansionist tendencies, the set of abnormal/matrix boundaries over which $\langle |v_{am}(t)| \rangle_i$ is calculated will have been exchanged against an entirely disjoint set. This GB-level analysis illustrates the fundamental quandary of AGG: If the phenomenon is truly governed by characteristics of the GB network and not the abnormal grains themselves, then how is it possible for faster growth to persist with a constantly changing set of abnormal/matrix GBs? In other words, having solved the problem of the growth advantage, we are left with the puzzle of persistence.

2.4. Observing Abnormal Grain Growth in Polycrystals

Experimental observations capture the various morphologies of abnormal grains (as evinced in Figure 1) but are limited in their ability to reveal the mechanisms by which the grains evolve. The fraction of grains that may undergo AGG depends on the system, typically ranging from 1 in 20,000 grains to as few as 1 in 1,000,000. Thus, it is not feasible to image sample regions of sufficient size and resolution to capture AGG in situ. After a specimen has been processed, it may be apparent that AGG has occurred, but the phenomenon tends to cover its tracks, as the rapid growth of an abnormal grain consumes its original neighborhood. This eradicates any aspects of the initial microstructural state that may have fostered abnormal grain evolution. Nonetheless, experimental observations have provided circumstantial (and sometimes contradictory) evidence regarding the mechanisms of AGG. Below, we review a representative selection of observations.

In 1935, Goss (108) reported an annealing and cold-rolling procedure that produced grainoriented Fe-3 wt% Si steels having enhanced magnetic properties. This finding was attributed to the strength of the {110}(001) texture, which has since been named the Goss texture. In silicon steels, the Goss texture develops as Goss grains emerge by AGG, taking on characteristic shapes





⁶Abnormally fast GB migration does not automatically entail rapid growth of a grain bounded by abnormal/ matrix interfaces, as the net result could instead be shrinkage of the grain in question. Persistence of the latter case, however, invariably leads to grain disappearance, leaving behind only those abnormal grains that persist in growing.

with peninsulas and island grains, as shown in Figure 1g,i,j. Owing to their high magnetic permeability and low hysteresis losses, Goss-textured silicon steels are still used in transformers and other electrical components (109). However, the mechanism of microstructural evolution during processing of these materials has yet to be established and is still a topic of active debate (11, 79, 109-111).

Texture-driven AGG, sometimes called abnormal subgrain growth, has been identified in materials with highly mobile subgrain boundaries. Ferry & Humphreys (76) fabricated a Goss-oriented single-crystalline Al–Si alloy and subjected it to compression deformation. The subgrain structure of the resulting material was characterized by X-ray diffraction to confirm that no high-angle GBs were formed during deformation. After annealing, abnormally large subgrains were found. The morphology of these abnormal subgrains was found to include peninsular structures protruding into neighboring regions of the microstructure. Compared with smaller subgrains, the abnormal subgrains in the material were more highly misoriented with respect to their neighbors. Analysis of the kinetics of abnormal subgrain growth indicated that abnormal subgrains have GB mobilities about 14 times higher than those of typical subgrains, although other studies have found mobility advantages as great as 500 (60) or 10⁴ (59) times higher. An investigation of cold-rolled Goss-oriented single crystals of copper reported similar behavior (112).

The presence or absence of solutes or other impurities can cause a growth advantage for a subset of grains. Hau-Riege & Thompson (113) investigated room-temperature AGG in electroplated Cu films. Additives in the electroplating bath led to the incorporation of impurities in the growing film. It was proposed that solute drag from the impurities limits grain growth, yielding a nanocrystalline matrix into which a few grains grow abnormally. Fine-grained regions have a high density of GBs, providing a large driving force for grain growth and many pathways for fast diffusion of impurities. The abnormal grains were found to expel impurity atoms, unpinning adjacent GBs and allowing AGG to persist. However, the authors did not determine which factors led to impurity rejection or to the selection of certain grains as candidates for AGG, leaving these as open research questions.

The presence of solutes can also influence the trajectory of grain growth in ceramics. MacLaren et al. (9) investigated AGG in alumina doped with Y and Si. A thin disordered region, which was associated with the presence of Si and Y impurities, was found near the boundaries of abnormally large grains. Most likely owing to a higher rate of atomic diffusion, this disordered region is believed to increase the boundary mobility of the grains, thereby leading to AGG. Similar observations in doped ceramic materials have been attributed to GB complexions (8, 114). Complexions denote interfacial structures that exist in thermodynamic equilibrium with the bulk material surrounding the interface. They can undergo transitions during processing, influencing the energy and mobility of the interface. In a detailed review, Cantwell et al. (115) propose that dramatic differences in GB mobility between complexions can initiate the abnormal growth of certain grains, as in the material shown in **Figure 1***d*.

The atmosphere under which a specimen is processed can be associated with AGG. Betanda et al. (116) investigated the occurrence of AGG in a Ni-5 at% W alloy. In this material, the abnormal growth of randomly oriented grains suppresses the {100}(001) cube texture that is desired for the epitaxial growth of superconducting films. Significant AGG was found to occur at high temperatures when samples were heated under hydrogen gas but not when processed under an Ar atmosphere. In this case, AGG was attributed to the diffusion of hydrogen into the material, which increases the mobility of dislocations near GBs, thereby enhancing the mobility of the GBs themselves. In contrast, Lee et al. (117) studied the effect of the atmosphere on AGG in barium titanate, observing that AGG occurred when specimens were sintered in air but that processing the same material under hydrogen suppressed abnormal growth. GB faceting occurred under the



oxidizing atmosphere, but it was not observed for the reducing one. This suggests that chemical changes introduced significant anisotropy in the GB energy and/or mobility, thus promoting AGG in the material during annealing in air.

The presence of second-phase particles typically limits grain growth in accordance with the Zener pinning effect (93). Surprisingly, however, the same particles that usually oppose GB migration appear, in some circumstances, to actually trigger AGG (94). Dennis et al. (95) observed AGG (including island grains and grains with peninsula-shaped boundaries) in Al-3.5 wt% Cu containing CuAl₂ precipitates. Texture analysis indicated that there was no significant difference in texture for the abnormal grains. Instead, it was found that the volume fraction of pinning particles located on the boundaries of abnormal grains was about half that on the boundaries of the smaller grains in the matrix. The root cause of this reduced coverage of abnormal/matrix interfaces was not determined and remains an open question. Similar observations were reported for particle-pinned systems annealed near the particle solvus (96, 97). The dissolution of pinning particles below the solvus temperature can unpin some GBs, potentially enabling the occurrence of AGG. Finally, AGG has been observed in particle-pinned systems with a stable and uniform particle dispersion (98, 118). In this case, selective unpinning of GBs is attributed to random thermal fluctuations in the boundary position. Overall, experimental observations suggest that any mechanism that decreases particle pinning on some GBs while holding the remaining boundaries in place is a potential growth advantage mechanism for AGG.

In summary, AGG has been studied in a diverse set of materials systems, and it remains an active area of research with a number of unresolved issues. Texture, impurities, atmosphere, and secondphase particles have all been shown experimentally to contribute to AGG, demonstrating the wide range of potential mechanisms relevant to the phenomenon. A common theme, however, is the observation that the abnormal grains develop an initial growth advantage that persists as they grow, and in most cases the growth advantage is better understood than the persistence mechanism.

2.5. Investigating Abnormal Grain Growth via Computer Simulation

In order to investigate proposed AGG initiation and growth mechanisms, a variety of microstructural-scale computer simulations have been developed and applied. These simulations capture grain-scale phenomenology, including GB properties and connectivity. Because they are not mean-field models, they can resolve the effects of evolving grain environments as growth proceeds. However, as with all mesoscale models, the physics and model parameters are selected by the modeler, so there is no guarantee that the simulated system reproduces a physically attainable scenario.

The first microstructural-scale AGG simulations were conducted by Rollett et al. (52) in 1989 as part of a series of microstructural evolution studies that utilized the MCPM for grain growth. In agreement with the theoretical predictions of Thompson et al. (25), Rollett et al. (52) found that, in polycrystals with uniform GB energy and mobility (ideal grain growth), grains having an initial size advantage with respect to their neighbors do not undergo AGG. In contrast, candidate abnormal grains given a sufficiently large GB energy advantage relative to matrix grains ($\Gamma \leq 0.5$) grow abnormally, regardless of initial size. The authors of Reference 52 acknowledge, however, that this is an unlikely scenario [as previously noted by Nielsen (75)], since it requires the boundaries of the candidate grain to be low in energy and thus presumably have low misorientations with respect to the adjacent matrix grains, all of which share high-energy (i.e., high-misorientation) boundaries with each other. In addition, Rollett et al. (52) examined the case in which the GB energy is uniform but candidate grains were given a mobility advantage (M > 1) and size advantage. This situation leads to AGG, with the necessary mobility advantage decreasing as the initial size advantage is



made more pronounced. These results confirmed that, although a size advantage acting alone never results in persistent AGG, in conjunction with either energy or mobility advantages, AGG can indeed occur (provided the energy or mobility advantage persists as the candidate grain grows).

Holm et al. (119) expanded the MCPM-based examination of AGG to include polycrystals with realistic crystallography and boundary properties, specifically for the texture-driven casefor which there is existing theory in the literature (120). Incorporating experimentally observed texture, GB mobility, and GB energy functions into the simulations, these authors found that AGG occurs spontaneously (without preselecting candidate grains), whereby the grains that grow abnormally are characterized by having a large fraction of high-misorientation (thus, high-mobility) GBs. The prevalence of abnormal events is quantitatively related to the fraction of grains in the initial state that are highly misoriented with respect to the dominant texture component of the matrix, and the resulting abnormal grains grow with the same morphological characteristics—including peninsula-shaped boundaries and island grains—that are observed in experiment. By selectively turning off the GB energy and mobility functions, Holm et al. (119) found that nonuniform GB mobility was required for AGG to occur in this system but that anisotropic GB energy was not. DeCost & Holm (121) extended this work using a model system to examine how the fraction of high-mobility GBs affects the probability of AGG and the morphology of the resulting abnormal grains. Statistically similar results were obtained in 2D and 3D systems (121, 122), and the qualitative and quantitative results were replicated and further developed using the phase field model (PFM) by Liu et al. (123).

Simulations have also been applied to study the effects of pinning particles in AGG. The PFM has been used to simulate the influence of selective particle dissolution during carburization (124, 125). In this case, the spatial distribution of particles was found to affect the size and frequency of abnormal grains. Fjeldberg et al. (126) used MCPM simulations to investigate particle-assisted AGG. For polycrystals pinned by stable precipitates with uniform GB energy and mobility, AGG was observed to occur spontaneously after very long anneals. This was attributed to thermal fluctuations that detach a GB from its pinning particles. The newly mobile boundary triggers additional GB breakaway events, allowing the parent grain to grow into the matrix of pinned grains (127, 128). Other investigators have made similar observations in solute-pinned polycrystals using CA (102) and PFM (103, 104) models. In both particle-pinned and solute-pinned cases, the persistence mechanism (i.e., how an unpinned GB manages to avoid becoming repinned) is scarcely understood, in part owing to the extremely rapid migration of the abnormal/matrix interface following the initial unpinning event.

Concurrently with early MCPM studies, Frost, Thompson, and colleagues (26, 27) used a vertex model to simulate grain growth in thin films, including AGG driven by surface energy anisotropy. They showed that grains having low-energy free surfaces can grow persistently, provided that the matrix grains are characterized by predominantly higher-energy free surfaces, as can occur in highly textured films.

Ko and colleagues used MCPM (129) and PFM (77) simulations to demonstrate the SB-SSW mechanism for AGG. They showed that, under the thermodynamic assumptions of the SB-SSW model, subgrain boundaries can assist in AGG and that the resulting abnormal grains share certain morphological characteristics with experimentally observed Goss grains in Si steels. However, since the GB energies were treated as input parameters to the simulations, the authors could not determine from these investigations how likely it is for the required energetic conditions to be met in real polycrystals.

Similarly, Frazier et al. (130) used MCPM to simulate AGG in a polycrystalline microstructure with GB complexions of differing energy and/or mobility. Abnormal grains were observed to grow, and the process resembled experimentally observed AGG in alumina–silica ceramics. However, for

15.14 Krill et al.



AGG to persist, the authors had to make rather arbitrary assumptions about the manner in which complexions are carried along as the growing abnormal grain encounters new neighbors.

To our knowledge, large-scale computer simulations have yet to be carried out for decoupled AGG in solid-state polycrystals, although the PFM has been applied to study highly faceted crystal growth in liquids (131) and during phase transformations (132).

Overall, we see that a variety of AGG scenarios have been examined using computational modeling and simulation. Simulations have provided key evidence supporting the feasibility (or lack thereof) of proposed mechanisms for the growth advantage during AGG, including GB energy, GB mobility, and particle pinning. A caveat to keep in mind is the fact that the physical realism of the grain growth simulations is determined by the underlying physical models and their selected parameter values. A great benefit of computational modeling is its ability to examine the AGG persistence mechanism, owing to the possibility of storing the system configuration at each time step. Not every study has been able to capitalize on this feature, however, due to the many challenges inherent to a time-resolved analysis of such large data sets.

3. DISCUSSION

3.1. Classifying Abnormal Grain Growth on the Basis of Morphological Features

As is evident in Figure 2, by introducing various growth advantages into Equation 1, we are able to simulate a variety of abnormal grain shapes. To the extent that the morphological features are characteristic of the assumed equation of motion, we can use them to classify observed instances of AGG into one of several categories, each of which is correlated with a particular growth advantage. One possible classification scheme is illustrated in Figure 3, which focuses on two attributes of the interface between an abnormally growing grain (a) and its surrounding matrix grains (m). First, the dihedral angle θ formed by the abnormal grain at a/m/m triple junctions is examined in a 2D section of the a/m interface. A value of $\theta = 180^{\circ}$ corresponds to an abnormal grain having flat facets, indicative of decoupled growth of the a grain (Figure 2)—typically, via the formation of a boundary phase or complexion (115). The presence of such a phase or complexion state along the faces of the a grain permits energy minimization of the latter independently of the shape and/or orientation of neighboring m grains, thus favoring the exposure of low-energy, high-symmetry crystal planes.

At the opposite extreme lies the case of dihedral angles $\theta \approx 0^{\circ}$, which occurs, for instance, during wetting by a liquid phase along a GB or triple junction. It has been proposed that the same mechanism can occur in solid materials when at least some a/m boundaries have much lower energy than m/m boundaries (79, 133). The key morphological feature of GB energy-governed AGG is the presence of particularly acute angles at triple junctions along the perimeter of the abnormal grain, as demonstrated in the second column of Figure 2. It is important to note, however, that a triple junction is a 3D object: Depending on the orientation of the plane in which an a/m/m junction is imaged (e.g., the specimen surface or a 2D section passing through the junction), the apparent value of θ can differ drastically from its true value in 3D. Care must therefore be taken to rule out stereological effects when assessing whether low GB energies contribute to a particular instance of AGG. Furthermore, as discussed in Section 2.2.1, polycrystalline configurations that would enable persistent GB energy-governed AGG have yet to be convincingly identified.

Most typically, θ takes on intermediate values between those associated with prismatic growth or wetting—i.e., $0^{\circ} \ll \theta \ll 180^{\circ}$. Here, a second criterion can assist in distinguishing between two additional forms of AGG. Except for the flat boundaries characteristic of decoupled AGG, the perimeter of an abnormal grain manifests shape fluctuations on the length scale of the average





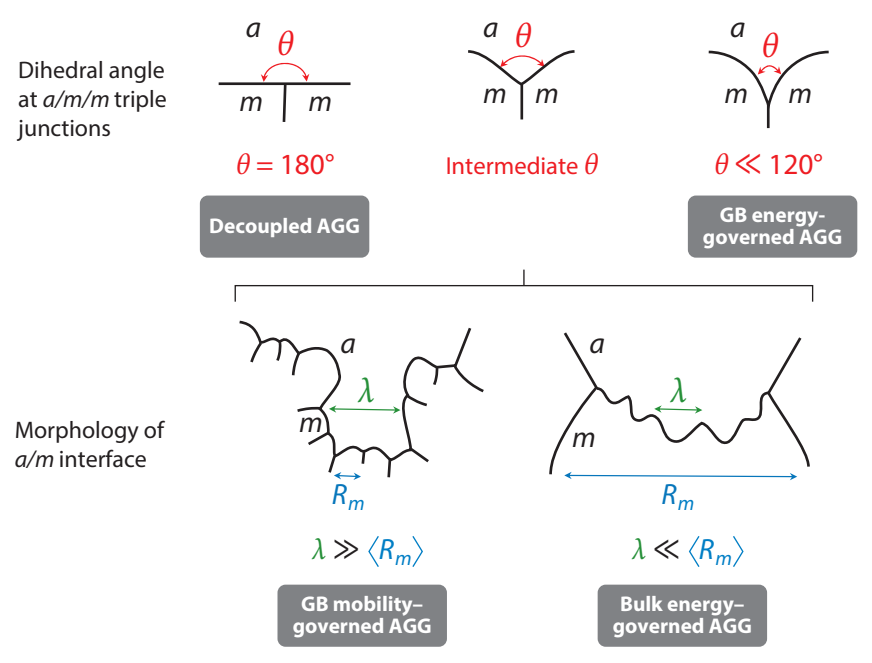


Figure 3

Two-step scheme for classifying abnormal grain growth (AGG) on the basis of morphological features of the interface between an abnormal grain (a) and matrix grains (m). Extreme values of the dihedral angle θ formed at a/m/m triple junctions permit decoupled AGG to be distinguished from AGG governed by anisotropy in grain boundary (GB) energy. When θ takes on intermediate values, AGG is likely to have resulted from GB mobility variations or from a bulk energy contribution. The latter two cases can be separated on the basis of whether the characteristic length λ of fluctuations in the a/m interface is larger or smaller than the average matrix grain size, $\langle R_m \rangle$.

matrix grain size $\langle R_{\rm m} \rangle$; these arise from the establishment of local equilibrium at the triple junctions along the abnormal/matrix interface. Additional spatial fluctuations may be present at another characteristic length scale, λ , as well. For example, when grain growth is driven by a bulk energy contribution, fluctuations at a scale smaller than the matrix grain size (i.e., $\lambda \ll \langle R_{\rm m} \rangle$) are frequently observed, as illustrated in the rightmost column of Figure 2. The microstructural signature of bulk energy-governed AGG is wavy or noncompact GBs along the perimeter of the abnormal grain. Such a morphology may form when spatial gradients in the bulk driving force exceed the curvature-based driving force of Equation 1, thereby overcoming the flattening effect of curvature-driven GB migration. Consequently, this form of AGG is generally associated with recrystallization, but it can also be caused by other volumetric driving forces.

Figure 1g-l reveals an interface morphology that seems to arise when neither decoupling nor gradients in bulk energy govern grain growth; in this case, the a/m boundary manifests fluctuations with a characteristic length scale significantly greater than the matrix grain size ($\lambda \gg \langle R_{\rm m} \rangle$). Qualitatively, a GB mobility-governed AGG microstructure is marked by the presence of protrusions (i.e., peninsula-shaped regions) extending out from the abnormal grain into the matrix (center column of Figure 2). It is tempting to attribute these protrusions to a kind of penetration mechanism occurring in a medium defined by the matrix, whereby an abnormal grain preferentially consumes a certain subset of the matrix grains upon which it impinges. Of course, for such a mechanism to persist, the volume fraction of matrix occupied by the rapidly consumable grains



must be sufficient to sustain abnormal growth. Beyond that point, depending on the precise value of this volume fraction, we might expect the boundaries of the abnormal grain to migrate in a more or less dendritic manner.

3.2. Morphological Signature of Abnormal Grain Growth Governed by Grain Boundary Mobility Variations

This penetration model was put to the test by DeCost & Holm (121), who simulated the growth of an abnormal grain into a polycrystalline matrix for different fractions of high-versus low-mobility GBs. As the fraction of high-mobility GBs was increased from zero to about 0.8, protrusions along the abnormal grain perimeter were found to be increasingly prevalent (top row of **Figure 4**). The authors quantified this trend in terms of a geometric characteristic proposed by Mason et al. (134): The circularity C of a grain is calculated from its perimeter P and area A according to $C = 4\pi A/P^2$. The maximum possible circularity, C = 1, corresponds to a grain having a perfectly circular cross section. Because any kind of protrusion raises P relative to the perimeter of a circle of equal A, the circularity of even normal grains lies below 0.9 due to the presence of triple junctions, and abnormal grains manifest still lower values for C. Since the frequency and size of peninsular features increases with the fraction of high-mobility GBs, abnormal grain circularity decreases with high-mobility fraction down to $C \approx 0.1$. The convoluted boundaries of low-C grains were also observed to migrate much faster through some neighboring matrix grains than others, resulting in the enclosure of island grains. Hence, the telltale morphological signs of GB mobility variations appear to be the low circularity values of abnormal grain cross sections and the (transient) presence of fully enclosed matrix grains behind the advancing a/m interfaces.

Peninsulas and island grains are both caused by matrix grains that an abnormal grain is unable to consume quickly; that is, they are grains that share low-mobility boundaries with the abnormal grain and thus block its progress. As the high-mobility boundary fraction is increased, however, there are fewer such blocking grains. At the largest fractions of high-mobility GBs, the trend of decreasing circularity is reversed: The abnormal grain expands uniformly without the formation of peninsulas and island grains, as illustrated in Figure 4 when the high-mobility fraction approaches unity. This situation can be distinguished from the normal growth case (high-mobility fraction of zero)—which also results in a relatively circular grain—by the extreme size achieved by the abnormal grain relative to the matrix.

Experimentally, the growth of GB protrusions and the appearance of island grains are both well established during AGG (110, 121, 137–139), although abnormal grain circularity measurements have not been reported for experimental systems. In Figure 4, we show circularity values calculated for the abnormal grains of **Figure 1** as well as related microstructures. We find that C varies with the material in question but that, for a given alloy, abnormal grains take on consistent and repeatable circularity values (i.e., small error bars), even between studies performed by different investigators. In addition to the qualitative resemblance between simulated and experimental abnormal grains, their circularity values are found to be comparable, as is evident in Figure 4, where simulated (top) and experimental (right) structures appear on the same graph. Although we do not know the fraction of high-mobility a/m boundaries (or the range of GB mobility values) for most experimental systems, the apparent agreement with simulation suggests a common mechanism. A tantalizing implication of this finding could be an explanation for the AGG that has been reported to occur in diverse systems, including in the presence of pinning particles, solute drag,





⁷ Notably, island grains typically have low-misorientation (thus, presumably low-mobility) boundaries with the abnormal grain (137), consistent with a mobility-governed AGG mechanism.

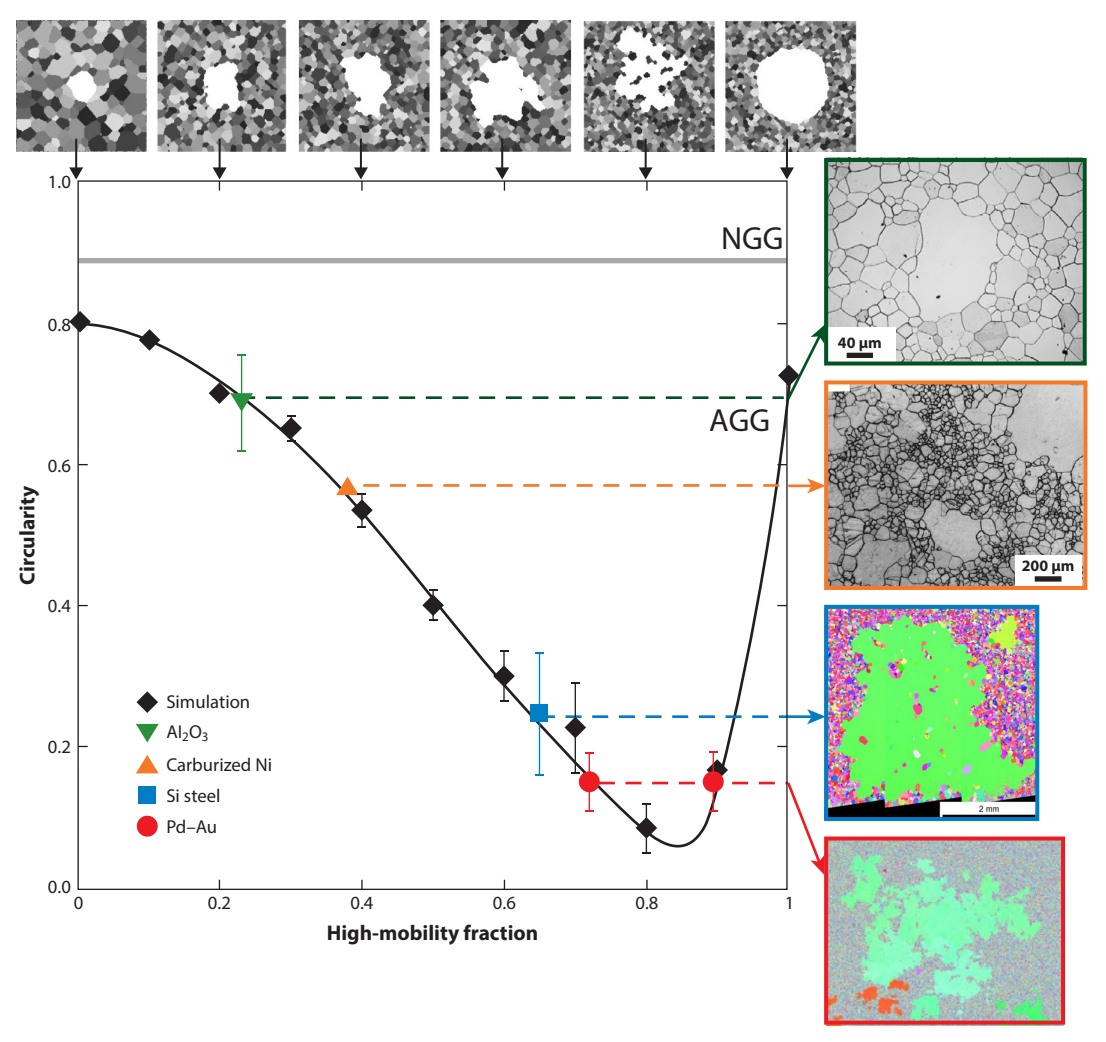


Figure 4

The dependence of abnormal grain morphology (circularity) as a function of the fraction of high-mobility a/m boundaries. Black diamonds and the top row of images give the MCPM simulation results of DeCost & Holm (121). Other symbols indicate circularity measurements we made of experimentally observed abnormal grains, with example images shown in the right column for Al₂O₃ (8, 9, 114), carburized Ni (10), Si steel (11, 13, 14, 105), and Pd–Au (135, 136). High-mobility fractions are not known for the experimental systems; the circularity data points are placed along the *x*-axis to best coincide with the simulation data. The solid gray line indicates the circularity of normal matrix grains, and the black curve is a guide for the eye. Error bars represent the standard deviation in circularity for a group of observations and simulations. The simulated and experimental abnormal grains strongly resemble each other both in visual appearance and measured circularity. Top row of images adapted with permission from Reference 121 with permission from Springer Nature. Micrograph for Al₂O₃ reproduced from Reference 8 with permission from Elsevier, for carburized Ni from Reference 10 with permission from Springer Nature, for Si steel from Reference 13 with permission from Elsevier, and for Pd–Au from Reference 136 (CC BY 3.0). Abbreviations: AGG, abnormal grain growth; MCPM, Monte Carlo Potts model; NGG, normal grain growth.

GB complexions, and even crystalline texture: These growth advantages could all trigger AGG merely by inducing sufficiently strong variations in mobility from one GB to the next.

If the morphological agreement between simulation and experiment can indeed be attributed to an underlying physical similarity, then **Figure 4** offers a way to interpret experimental

15.18 Krill et al.



observations. Given a measured abnormal grain circularity, Figure 4 associates that value for C with a fraction of high-mobility a/m boundaries on the abnormal grain. For example, the average circularity of Si steel abnormal grains, $\langle C \rangle = 0.25 \pm 0.09$, corresponds to a high-mobility boundary fraction of about 0.65. This is within the experimentally observed range, as reported by Rajmohan & Szpunar (140). This method can also help select among models for AGG. For instance, the average circularity of abnormal Al₂O₃ grains growing by the complexion mechanism is $\langle C \rangle = 0.69 \pm 0.07$; this corresponds to a high-mobility boundary fraction of either 0.23 or almost 1.0. Examining the simulated grains visually, we see that the abnormal grain with a high-mobility fraction of 0.2 more closely resembles the experimental abnormal grain, so the more likely high-mobility fraction is the lower one. In the case of highly noncircular abnormal grains, such as the Pd-Au grains in Figure 4, the choice between the two intercepts may be ambiguous; in this case, both possible high-mobility fractions are shown on the graph.

A further piece of evidence in support of holding variations in GB mobility responsible for the abnormal growth of irregular grain morphologies can be gleaned from time-resolved studies of a/m interface migration in experiment and simulation. The jerky motion reported by Hutchinson (139) for AGG in a silicon steel matches DeCost & Holm's (121) simulations of a/m interface migration through a matrix with a wide range of GB mobilities, whereby the qualitative agreement holds in both the spatial and temporal domains, as shown in Figure 5.

3.3. Understanding the Persistence of Grain Boundary Mobility-Governed **Abnormal Grain Growth**

The microstructural correlations evident in Figures 4 and 5 make a reasonably strong case for attributing the most commonly observed morphological features of extreme AGG—the suppression of grain circularity and the appearance of island grains, both occurring without signs of sharp dihedral angles mediated by GB energetics—to a nonuniform distribution of GB mobilities in a polycrystalline microstructure. It remains challenging, however, to explain how this mobility distribution forms and, critically, how it enables persistent growth of the abnormal grain at the expense of the matrix grains. Why, for instance, does a broad spectrum of mobility values exert a profound effect on the growth kinetics of a/m interfaces but not on the behavior of the much more prevalent m/m boundaries between matrix grains? The translation of a given GB requires only small displacements of atoms located in and near the GB core (85). If the core regions of m/m and a/m interfaces are statistically identical at the atomic level, then how is it possible for these two classes of GBs to migrate so differently? If, on the other hand, the atomic environments are not statistically identical—for example, in cases in which solute segregation or particle pinning turns out to be more extensive at m/m interfaces—then the challenge consists of explaining not only the origin of this difference but also its persistence as a/m interfaces advance through the matrix.

The morphological analysis carried out in this review highlights the central role played by GB mobility in AGG—of course, without being able to unravel the atomistics of the phenomenon. Surprisingly, this places our understanding of AGG roughly on par with that of the purportedly much simpler case of normal grain growth. Recent attempts to model the evolution of polycrystalline microstructures in terms of GB disconnections—line defects in GBs that are analogous to dislocations in bulk crystals (84)—have called attention to the plethora of atomic-level structures and processes that are subsumed under the proportionality constant μ in Equation 1 (90, 141). The long-range translation of an a/m interface necessarily entails sustained migration of disconnections to and from a/m/m triple junctions, where reactions with other disconnections can occur, disconnections may be annihilated, or new ones may be generated. Such events are likely to constitute the rate-limiting step for GB migration. It is conceivable that the key feature that



14:43

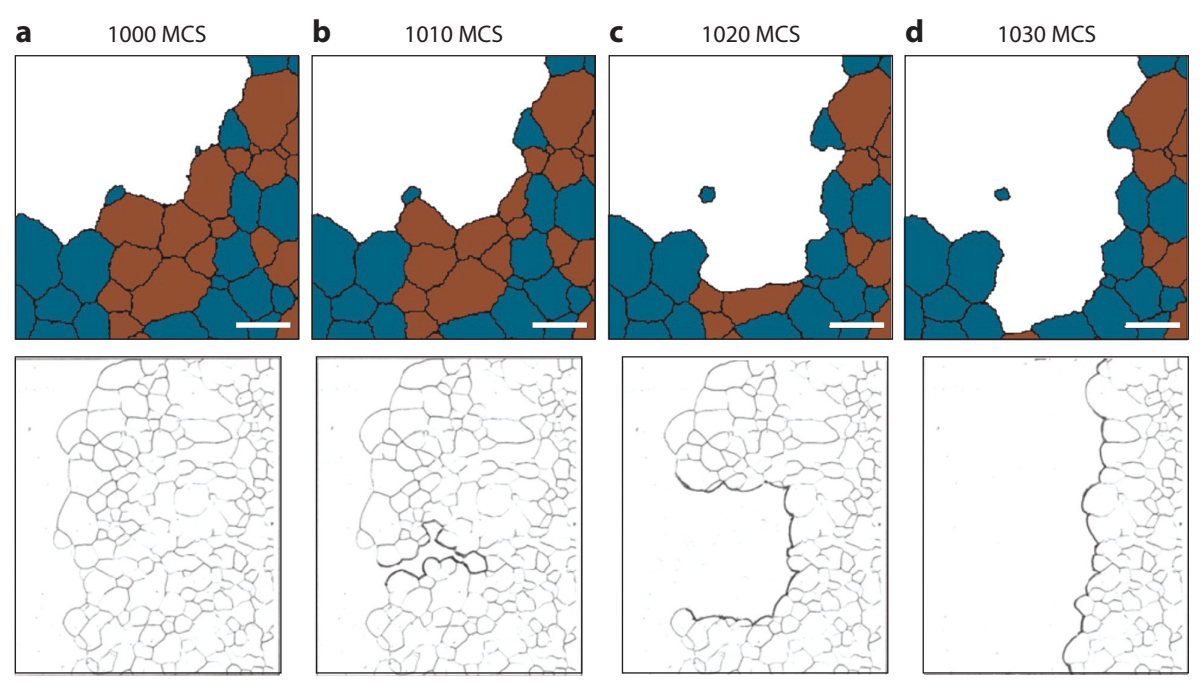


Figure 5

AGG by the penetration mechanism. The top row of images shows a time series from the simulations of DeCost & Holm (121). The white abnormal grain grows by consuming grains with which it shares high-mobility boundaries (*brown*). In doing so, it penetrates into the matrix and leaves behind an island grain and peninsular structures. The bottom row of images shows the schematic of a time sequence of AGG in Si steel, as observed in scanning electron microscopy by Hutchinson (139). Analogously to the simulation results, the abnormal grain penetrates the matrix by consuming a group of matrix grains and then expands outward, creating peninsular features. White scale bars represent 50 pixels in the simulation cell. Top row of images adapted from Reference 121 with permission from Springer Nature. Bottom row of images adapted from Reference 139 with permission from Trans Tech Publications. Abbreviations: AGG, abnormal grain growth; MCS, Monte Carlo time step.

distinguishes AGG from its normal counterpart is the spatial homogeneity of the kinetics of disconnection generation, propagation, and annihilation in a given microstructure. If this hypothesis is correct, then future investigations ought to focus on elucidating the ways in which disconnections can interact with microstructural features to promote what we have identified mesoscopically as AGG governed by variations in GB mobility.

4. CONCLUSIONS

This review has assessed AGG from a phenomenological standpoint, starting from the necessary conditions for rapid and sustained growth of a subpopulation of grains and relating potential mechanisms to the corresponding morphology of a/m interfaces. The following conclusions can be drawn from this analysis.

1. When grain growth is driven by the reduction of excess free energy stored in the GBs, the phenomenon is most appropriately viewed as taking place on the GB network, even though abnormally fast growth appears to be characteristic of an entire grain. For this reason, the conditions for AGG should be formulated in terms of the migration rates v^{GB} of individual GBs rather than the growth rates of grains.

15.20 Krill et al.



- 2. For AGG to take place, not only must a/m GBs migrate much faster than m/m GBs, but so too must this growth advantage be sustained, despite the abnormally growing grains continually impinging upon new matrix neighbors (persistence).
- 3. The Burke-Turnbull expression for the GB equation of motion, $v^{GB} = \mu \gamma \kappa$, provides a useful framework for classifying possible growth advantages. If all GBs share the same mobility μ and energy γ values, grain growth proceeds in a normal manner; consequently, AGG cannot be encoded solely in the curvature κ . Only GB-to-GB variations in μ and/or γ can lead to fulfillment of the growth advantage criterion, as verified by computer simulation.
- 4. When models for μ or γ anisotropy are indexed to specific properties of an a/m GB (such as its misorientation angle, the Σ -value of the coincidence site lattice, or the boundary inclination), it is problematic to account for the persistence of AGG, since the aforementioned quantities change abruptly each time an abnormally growing grain encounters a new neighbor in the matrix. A complete model for AGG must explain not only the genesis of the growth advantage but also the manner in which it is maintained during long-range migration of a/m GBs.
- 5. Insight into the mechanism underlying the operative growth advantage can be extracted from the morphology of the a/m interface. This interface is most amenable to examination in cases of extreme AGG, which we define somewhat arbitrarily as having occurred when the abnormal subpopulation of grains reaches sizes at least an order of magnitude larger than those of its matrix counterpart.
- 6. The dihedral angle at a/m/m triple junctions distinguishes prismatic AGG (decoupled) and AGG governed by γ -anisotropy from AGG driven by bulk energy terms or variations in μ (Figure 3). Discrimination between the latter two cases is possible on the basis of the characteristic length of fluctuations along the a/m interface.
- 7. When not classified as decoupled, most documented cases of extreme AGG appear to be enabled by variations in the GB mobility. The entire range of experimentally observed grain circularities (a measure for the deviation of a grain's cross section from that of an equal-area circle) is found to be consistent with computer simulations carried out under the assumption that abnormally growing grains have a high value for μ when in contact with a certain fraction of matrix grains but low mobility with the rest. The greater this fraction, the more convoluted is the shape of the a/m interface, suggesting that the greatest discrepancy from compact grain shapes (i.e., low circularity) is caused by a mechanism that suppresses the mobility of about 15 to 20% of the GBs bordering the abnormal grain (but nearly all GBs within the matrix).
- 8. Although a high- or low-mobility model adequately accounts for the wide range of observed abnormal grain morphologies, it is not obvious how specific components of a polycrystalline material's microstructure are able to establish such a dichotomy in the spectrum of μ values. Open questions include the following:
 - a. How is it that many a/m GBs are capable of taking on a higher value of mobility, but very few if any of the m/m GBs share this ability?
 - b. Can atomic-level structural and/or compositional differences in the core regions of a/m and m/m interfaces account for the discrepancy in their characteristic GB mobilities?
 - c. How does an a/m interface maintain its mobility advantage as it sweeps through new regions of the matrix?

Potential answers to these unresolved issues will have to encompass the influence of pinning particles and GB segregants as well as GB complexions, as each of these microstructural features can be intimately associated with AGG. In all three cases, the challenge posed by the observed





persistence of the phenomenon appears to be the most formidable. New insights into this particular aspect could possibly be gained from ongoing studies of the fundamental role played by GB disconnections during GB migration.

DISCLOSURE STATEMENT

The authors are not aware of any affiliations, memberships, funding or financial holdings that might be perceived as affecting the objectivity of this review.

ACKNOWLEDGMENTS

We thank Marc Bernacki, Håkan Hallberg, Matthias Militzer, and Gregory Rohrer for insightful discussions of the phenomenon of AGG as well as for drawing our attention to relevant publications. Furthermore, we express our gratitude to Jörg Schmauch for acquiring the high-resolution electron backscatter diffraction images of Pd-Au shown in Figures 1 and 4. The authors from Ulm gratefully acknowledge research funding provided by the Deutsche Forschungsgemeinschaft through grants KR 1658/9-1 (to C.E.K., J.M.D., and K.H.) and KR 1658/10-1 (to C.E.K., J.M.D., and F.A.). E.A.H. and R.C. were supported by the US National Science Foundation grants CMMI-1826218 and DMR-2118945 and the United States Air Force D3OM2S Center of Excellence under agreement FA8650-19-2-5209.

LITERATURE CITED

- 1. Dunn CG, Walter JL. 1966. Secondary recrystallization. In Recrystallization, Grain Growth and Textures, pp. 461-521. Metals Park, OH: Am. Soc. Metals
- 2. Humphreys J, Rohrer GS, Rollett A. 2017. Grain growth following recrystallization. In Recrystallization and Related Annealing Phenomena, ed. J Humphreys, GS Rohrer, A Rollett, pp. 375-429. Oxford, UK: Elsevier, 3rd ed.
- 3. Raabe D. 2014. Recovery and recrystallization: phenomena, physics, models, simulation. In Physical Metallurgy, ed. DE Laughlin, K Hono, pp. 2291-397. Oxford, UK: Elsevier
- 4. Lawrence A, Rickman JM, Harmer MP, Rollett AD. 2016. Parsing abnormal grain growth. Acta Mater.
- 5. Kwon O, Hong S, Lee J, Chung U, Kim D, Hwang NM. 2002. Microstructural evolution during sintering of TiO2/SiO2-doped alumina: mechanism of anisotropic abnormal grain growth. Acta Mater. 50:4865-72
- 6. Zhao BB. 2015. Abnormal grain growth with {1 0 0} planar interface in the electrodeposited nickel. Mater. Res. Innov. 19:S251-54
- 7. Fisher JG, Lee BK, Brancquart A, Choi SY, Kang SJL. 2005. Effect of Al₂O₃ dopant on abnormal grain growth in BaTiO₃. 7. Eur. Ceram. Soc. 25:2033-36
- Dillon SJ, Tang M, Carter WC, Harmer MP. 2007. Complexion: a new concept for kinetic engineering in materials science. Acta Mater. 55:6208-18
- MacLaren I, Cannon RM, Gülgün MA, Voytovych R, Popescu-Pogrion N, et al. 2003. Abnormal grain growth in alumina: synergistic effects of yttria and silica. 7. Am. Ceram. Soc. 86:650-59
- 10. Lee SB, Hwang NM, Yoon DY, Henry MF. 2000. Grain boundary faceting and abnormal grain growth in nickel, Metall, Mater, Trans, A 31:985-94
- 11. Zaefferer S, Chen N. 2005. The Goss texture formation in silicon steels growth selection or oriented nucleation. Solid State Phenom. 105:29-36
- 12. Park HK, Kang HG, Park CS, Huh MY, Hwang NM. 2012. Ex situ observation of microstructure evolution during abnormal grain growth in aluminum alloy. Metall. Mater. Trans. A 43:5218–23
- 13. Kim TY, Na TW, Shim HS, Gil K, Hwang NM. 2022. Effect of the magnitude of sub-boundary angles on the abnormal grain growth rate of Goss grains in Fe-3%Si steel. Mater. Char. 184:111655
- 14. Park H, Kim DY, Hwang NM, Joo YC, Han CH, Kim JK. 2004. Microstructural evidence of abnormal grain growth by solid-state wetting in Fe-3%Si steel. 7. Appl. Phys. 95:5515–21



- 15. Fischer M. 2021. Investigation and analysis of microstructural evolution in nanocrystalline Pd_{100-x}Au_x. MA thesis, Universität Ulm, Ulm, Ger,
- 16. Greiser J, Müllner P, Arzt E. 2001. Abnormal growth of "giant" grains in silver thin films. Acta Mater. 49:1041-50
- 17. Nielsen JP. 1966. The grain coalescence theory. In Recrystallization, Grain Growth and Textures, pp. 141-64. Metals Park, OH: Am. Soc. Metals
- 18. Thompson CV, Smith HI. 1984. Surface-energy-driven secondary grain growth in ultrathin (<100 nm) films of silicon. Appl. Phys. Lett. 44:603-5
- 19. Hennings DFK, Janssen R, Reynen PJL. 1987. Control of liquid-phase-enhanced discontinuous grain growth in barium titanate. J. Am. Ceram. Soc. 70:23-27
- 20. Stöckhert B, Duyster J. 1999. Discontinuous grain growth in recrystallised vein quartz—implications for grain boundary structure, grain boundary mobility, crystallographic preferred orientation, and stress history. J. Struct. Geol. 21:1477-90
- 21. Gianola DS, Van Petegem S, Legros M, Brandstetter S, Van Swygenhoven H, Hemker KJ. 2006. Stress-assisted discontinuous grain growth and its effect on the deformation behavior of nanocrystalline aluminum thin films. Acta Mater. 54:2253-63
- 22. Duan J, Wen H, Zhou C, He X, Islamgaliev R, Valiev R. 2020. Discontinuous grain growth in an equalchannel angular pressing processed Fe-9Cr steel with a heterogeneous microstructure. Mater. Charact.
- 23. Na SM, Flatau AB. 2007. Secondary recrystallization, crystallographic texture and magnetostriction in rolled Fe-Ga based alloys. J. Appl. Phys. 101:09N518
- 24. Hayakawa Y. 2017. Mechanism of secondary recrystallization of Goss grains in grain-oriented electrical steel. Sci. Technol. Adv. Mater. 18:480-97
- 25. Thompson CV, Frost HJ, Spaepen F. 1987. The relative rates of secondary and normal grain growth. Acta Metall. 35:887-90
- 26. Frost HJ, Thompson CV. 1988. Computer simulation of microstructural evolution in thin films. J. Electron. Mater. 17:447-58
- 27. Frost HJ, Thompson CV, Walton DT. 1992. Simulation of thin film grain structures—II. abnormal grain growth. Acta Metall. Mater. 40:779-93
- 28. Ciulik J, Taleff EM. 2009. Dynamic abnormal grain growth: a new method to produce single crystals. Scr. Mater. 61:895-98
- 29. Dake JM, Krill CE. 2012. Sudden loss of thermal stability in Fe-based nanocrystalline alloys. Scr. Mater. 66:390-93
- 30. Chen S, Wang W, Kono H, Sassa K, Asai S. 2010. Abnormal grain growth of hydroxyapatite ceramic sintered in a high magnetic field. 7. Cryst. Growth 312:323-26
- 31. Hansen N. 2004. Hall-Petch relation and boundary strengthening. Scr. Mater. 51:801-6
- 32. Furnish TA, Bufford DC, Ren F, Mehta A, Hattar K, Boyce BL. 2018. Evidence that abnormal grain growth precedes fatigue crack initiation in nanocrystalline Ni-Fe. Scr. Mater. 143:15-19
- 33. Kingery WD, Bowen HK, Uhlmann DR. 1976. Introduction to Ceramics. New York: Wiley-Interscience
- 34. Ouhiba S, Nicolay A, Boissonnet L, Bernacki M, Bozzolo N. 2022. Formation of coarse recrystallized grains in 6016 aluminum alloy during holding after hot deformation. Metall. Mater. Trans. A 53:2402-25
- 35. Engler O, Hirsch J. 2002. Texture control by thermomechanical processing of AA6xxx Al-Mg-Si sheet alloys for automotive applications—a review. Mater. Sci. Eng. A 336:249-62
- 36. Lingk C, Gross ME. 1998. Recrystallization kinetics of electroplated Cu in damascene trenches at room temperature. 7. Appl. Phys. 84:5547-53
- 37. Lu CL, Lin HW, Liu CM, Huang YS, Lu TL, et al. 2014. Extremely anisotropic single-crystal growth in nanotwinned copper. NPG Asia Mater. 6:e135
- 38. Matsuo M. 1989. Texture control in the production of grain oriented silicon steels. ISI7 Int. 29:809-27
- 39. Su C, Zhao G, Xiao H, Lan Y, Huang F. 2018. Abnormal grain growth of Hi-B steel in the secondary recrystallization. Metallogr. Microstruct. Anal. 7:608-17
- 40. Vollmer M, Arold T, Kriegel MJ, Klemm V, Degener S, et al. 2019. Promoting abnormal grain growth in Fe-based shape memory alloys through compositional adjustments. Nat. Commun. 10:2337





- 41. Na SM, Atwater KM, Flatau AB. 2015. Particle pinning force thresholds for promoting abnormal grain growth in magnetostrictive Fe-Ga alloy sheets. Scr. Mater. 100:1-4
- 42. Hanaor DAH, Xu W, Ferry M, Sorrell CC. 2012. Abnormal grain growth of rutile TiO2 induced by ZrSiO₄. 7. Cryst. Growth 359:83-91
- 43. Wang Y, Chen M, Zhou F, Ma E. 2002. High tensile ductility in a nanostructured metal. Nature 419:912–
- 44. Ma E, Zhu T. 2017. Towards strength-ductility synergy through the design of heterogeneous nanostructures in metals. Mater. Today 20:323-31
- 45. Omori T, Kusama T, Kawata S, Ohnuma I, Sutou Y, et al. 2013. Abnormal grain growth induced by cyclic heat treatment. Science 341:1500-2
- 46. Noell PJ, Taleff EM. 2015. Dynamic abnormal grain growth in refractory metals. JOM 67:2642-45
- 47. Kusama T, Omori T, Saito T, Kise S, Tanaka T, et al. 2017. Ultra-large single crystals by abnormal grain growth. Nat. Commun. 8:354
- 48. Moore RD, Beecroft T, Rohrer GS, Barr CM, Homer ER, et al. 2021. The grain boundary stiffness and its impact on equilibrium shapes and boundary migration: analysis of the Σ 5, 7, 9, and 11 boundaries in Ni. Acta Mater. 218:117220
- 49. Sutoki T. 1928. On the mechanism of crystal growth by annealing. Sci. Rep. Tohoku Imp. Univ. 17:857-76
- 50. Burke JE, Turnbull D. 1952. Recrystallization and grain growth. Prog. Metal Phys. 3:220-92
- 51. Srolovitz DJ, Grest GS, Anderson MP. 1985. Computer simulation of grain growth—V. Abnormal grain growth. Acta Metall. 33:2233-47
- 52. Rollett AD, Srolovitz DJ, Anderson MP. 1989. Simulation and theory of abnormal grain growth anisotropic grain boundary energies and mobilities. Acta Metall. 37:1227-40
- 53. Grest GS, Anderson MP, Srolovitz DJ, Rollett AD. 1990. Abnormal grain growth in three dimensions. Scr. Metall. Mater. 24:661-65
- 54. Rollett AD, Mullins WW. 1997. On the growth of abnormal grains. Scr. Mater. 36:975-80
- 55. Rollett AD. 2005. Abnormal grain growth and texture development. Mater. Sci. Forum 495-97:1171-76
- 56. Rios PR. 1992. Abnormal grain growth in pure materials. Acta Metall. Mater. 40:2765-68
- 57. Taylor JE, Cahn JW, Handwerker CA. 1992. Overview no. 98 I—geometric models of crystal growth. Acta Metall. Mater. 40:1443-74
- 58. Gottstein G, Molodov DA, Shvindlerman LS, Srolovitz DJ, Winning M. 2001. Grain boundary migration: misorientation dependence. Curr. Opin. Solid State Mater. Sci. 5:9-14
- 59. Huang Y, Humphreys FJ. 2000. Subgrain growth and low angle boundary mobility in aluminium crystals of orientation {110} (001). Acta Mater. 48:2017–30
- 60. Huang Y, Humphreys FJ, Ferry M. 2000. The annealing behaviour of deformed cube-oriented aluminium single crystals. Acta Mater. 48:2543-56
- 61. Li J, Dillon SJ, Rohrer GS. 2009. Relative grain boundary area and energy distributions in nickel. Acta Mater. 57:4304-11
- 62. Olmsted DL, Foiles SM, Holm EA. 2009. Survey of computed grain boundary properties in face-centered cubic metals: I. Grain boundary energy. Acta Mater. 57:3694–703
- 63. Olmsted DL, Holm EA, Foiles SM. 2009. Survey of computed grain boundary properties in face-centered cubic metals—II: Grain boundary mobility. Acta Mater. 57:3704–13
- 64. Ratanaphan S, Olmsted DL, Bulatov VV, Holm EA, Rollett AD, Rohrer GS. 2015. Grain boundary energies in body-centered cubic metals. Acta Mater. 88:346–54
- 65. Ratanaphan S, Boonkird T, Sarochawikasit R, Beladi H, Barmak K, Rohrer GS. 2017. Atomistic simulations of grain boundary energies in tungsten. Mater. Lett. 186:116–18
- 66. Han J, Vitek V, Srolovitz DJ. 2016. Grain-boundary metastability and its statistical properties. Acta Mater. 104:259-73
- 67. He H, Ma S, Wang S. 2021. Survey of grain boundary energies in tungsten and beta-titanium at high temperature. Materials 15:156
- 68. Holm EA, Foiles SM. 2010. How grain growth stops: a mechanism for grain-growth stagnation in pure materials. Science 328:1138-41
- 69. Read WT, Shockley W. 1950. Dislocation models of crystal grain boundaries. Phys. Rev. 78:275-89



- 70. Sutton AP, Banks EP, Warwick AR. 2015. The five-dimensional parameter space of grain boundaries. Proc. R. Soc. A 471:20150442
- 71. Wagih M, Schuh CA. 2019. Spectrum of grain boundary segregation energies in a polycrystal. Acta Mater. 181:228-37
- 72. Barr CM, Foiles SM, Alkayyali M, Mahmood Y, Price PM, et al. 2021. The role of grain boundary character in solute segregation and thermal stability of nanocrystalline Pt-Au. Nanoscale 13:3552-63
- 73. Zhu Q, Samanta A, Li B, Rudd RE, Frolov T. 2018. Predicting phase behavior of grain boundaries with evolutionary search and machine learning. Nat. Commun. 9:467
- 74. Brandon DG. 1966. The structure of high-angle grain boundaries. Acta Metall. 14:1479-84
- 75. Nielsen JP. 1966. Some laws of grain growth. In Recrystallization, Grain Growth and Textures, pp. 286–94. Metals Park, OH: Am. Soc. Metals
- 76. Ferry M, Humphreys FJ. 1996. Discontinuous subgrain growth in deformed and annealed {110} (001) aluminium single crystals. Acta Mater. 44:1293-308
- 77. Ko KJ, Cha PR, Srolovitz D, Hwang NM. 2009. Abnormal grain growth induced by sub-boundaryenhanced solid-state wetting: analysis by phase-field model simulations. Acta Mater. 57:838-45
- 78. Ko KJ, Rollett AD, Hwang NM. 2010. Abnormal grain growth of Goss grains in Fe-3% Si steel driven by sub-boundary-enhanced solid-state wetting: analysis by Monte Carlo simulation. Acta Mater. 58:4414-23
- 79. Park CS, Na TW, Park HK, Kim DK, Han CH, Hwang NM. 2012. Misorientation characteristics of penetrating morphologies at the growth front of abnormally growing grains in aluminum alloy. Philos. Mag. Lett. 92:344-51
- 80. Omori T, Iwaizako H, Kainuma R. 2016. Abnormal grain growth induced by cyclic heat treatment in Fe-Mn-Al-Ni superelastic alloy. Mater. Des. 101:263-69
- 81. Pei R, Korte-Kerzel S, Al-Samman T. 2020. Normal and abnormal grain growth in magnesium: experimental observations and simulations. J. Mater. Sci. Technol. 50:257-70
- 82. Wolf D. 1990. A broken-bond model for grain boundaries in face-centered cubic metals. 7. Appl. Phys. 68:3221-36
- 83. Park YJ, Hwang NM, Yoon DY. 1996. Abnormal growth of faceted (WC) grains in a (Co) liquid matrix. Metall. Mater. Trans. A 27:2809-19
- 84. Han J, Thomas SL, Srolovitz DJ. 2018. Grain-boundary kinetics: a unified approach. Progress Mater. Sci. 98:386-476
- 85. Chesser I, Runnels B, Holm E. 2022. A taxonomy of grain boundary migration mechanisms via displacement texture characterization. Acta Mater. 222:117425
- 86. Kacher J, Eftink BP, Cui B, Robertson IM. 2014. Dislocation interactions with grain boundaries. Curr. Opin. Solid State Mater. Sci. 18:227-43
- 87. Barr CM, Chen EY, Nathaniel JE, Lu P, Adams DP, et al. 2022. Irradiation-induced grain boundary facet motion: in situ observations and atomic-scale mechanisms. Sci. Adv. 8:eabn0900
- 88. Huang Y, Humphreys FJ. 2012. The effect of solutes on grain boundary mobility during recrystallization and grain growth in some single-phase aluminium alloys. Mater. Chem. Phys. 132:166–74
- Dannenberg R, Stach EA, Groza JR, Dresser BJ. 2000. In-situ TEM observations of abnormal grain growth, coarsening, and substrate de-wetting in nanocrystalline Ag thin films. Thin Solid Films 370:54-62
- 90. Rohrer GS, Chesser I, Krause AR, Naghibzadeh K, Xu Z, et al. 2023. Grain boundary migration in polycrystals. Annu. Rev. Mater. Sci. 53. In press
- 91. Hillert M. 1965. On the theory of normal and abnormal grain growth. Acta Metall. 13:227-38
- 92. Gladman T, Allen NP. 1966. On the theory of the effect of precipitate particles on grain growth in metals. Proc. R. Soc. Lond. A 294:298-309
- 93. Smith CS. 1948. Grains, phases, and interfaces—an interpretation of microstructure. Trans. AIME 175:15-51
- 94. Humphreys FJ. 1997. A unified theory of recovery, recrystallization and grain growth, based on the stability and growth of cellular microstructures—II. The effect of second-phase particles. Acta Mater 45:5031-39
- 95. Dennis J, Bate P, Humphreys F. 2009. Abnormal grain growth in Al-3.5Cu. Acta Mater. 57:4539-47





14:43

- 96. Gangulee A, D'Heurle FM. 1972. Anomalous large grains in alloyed aluminum thin films I. Secondary grain growth in aluminum-copper films. Thin Solid Films 12:399-402
- 97. Uttarasak K, Chongchitnan W, Matsuda K, Chairuangsri T, Kajornchaiyakul J, Banjongprasert C. 2019. Evolution of Fe-containing intermetallic phases and abnormal grain growth in 6063 aluminum alloy during homogenization. Results Phys. 15:102535
- 98. Lu N, Kang J, Senabulya N, Keinan R, Gueninchault N, Shahani AJ. 2020. Dynamics of particle-assisted abnormal grain growth revealed through integrated three-dimensional microanalysis. Acta Mater. 195:1-
- 99. Trelewicz JR, Schuh CA. 2009. Grain boundary segregation and thermodynamically stable binary nanocrystalline alloys. Phys. Rev. B 79:094112
- 100. Cahn JW. 1962. The impurity-drag effect in grain boundary motion. Acta Metall. 10:789-98
- 101. Akiva R, Katsman A, Kaplan WD. 2014. Anisotropic grain boundary mobility in undoped and doped alumina. 7. Am. Ceram. Soc. 97:1610-18
- 102. Janssens KGF, Holm EA. 2005. On the interaction between a transient solute concentration at a moving grain boundary, precipitates and abnormal grain growth. Rep. SAND2005-0692C, Sandia Natl. Lab., Albuquerque, NM
- 103. Kim SG, Park YB. 2008. Grain boundary segregation, solute drag and abnormal grain growth. Acta Mater. 56:3739-53
- 104. Li J, Wang J, Yang G. 2010. Phase field simulation of grain growth with grain boundary segregation. Int. 7. Mater. Res. 101:555-59
- 105. Lee DK, Lee BJ, Ko KJ, Hwang NM. 2009. Comparison of the advantages conferred by mobility and energy of the grain boundary in inducing abnormal grain growth using Monte Carlo simulations. Mater. Trans. 50:2521-25
- 106. Hibbard GD, McCrea JL, Palumbo G, Aust KT, Erb U. 2002. An initial analysis of mechanisms leading to late stage abnormal grain growth in nanocrystalline Ni. Scr. Mater. 47:83-87
- 107. Moelans N, Godfrey A, Zhang Y, Juul Jensen D. 2013. Phase-field simulation study of the migration of recrystallization boundaries. Phys. Rev. B 88:054103
- 108. Goss PN. 1935. New development in electrical strip steels characterized by fine grain structure approaching the properties of a single crystal. Trans. Am. Soc. Metals 23:511-44
- 109. Xia Z, Kang Y, Wang Q. 2008. Developments in the production of grain-oriented electrical steel. J. Magn. Magn. Mater. 320:3229-33
- 110. Etter AL, Baudin T, Penelle R. 2002. Influence of the Goss grain environment during secondary recrystallisation of conventional grain oriented Fe-3%Si steels. Scr. Mater. 47:725-30
- 111. Morawiec A. 2011. On abnormal growth of Goss grains in grain-oriented silicon steel. Scr. Mater. 64:466-69
- 112. Ferry M, Humphreys FJ. 2006. Onset of abnormal subgrain growth in cold rolled {110} (001) oriented copper single crystals. Mater. Sci. Eng. A 435–36:447–52
- 113. Hau-Riege SP, Thompson CV. 2000. In situ transmission electron microscope studies of the kinetics of abnormal grain growth in electroplated copper films. Appl. Phys. Lett. 76:309-11
- 114. Dillon SJ, Harmer MP. 2008. Relating grain boundary complexion to grain boundary kinetics II: silicadoped alumina. 7. Am. Ceram. Soc. 91:2314-20
- 115. Cantwell PR, Tang M, Dillon SJ, Luo J, Rohrer GS, Harmer MP. 2014. Grain boundary complexions.
- 116. Betanda YA, Helbert AL, Brisset F, Waeckerlé T, Baudin T. 2015. Effect of annealing atmosphere on the recrystallized texture and abnormal grain growth of Ni-5%W alloy sheets. Adv. Eng. Mater. 17:1568-72
- 117. Lee BK, Chung SY, Kang SJL. 2000. Grain boundary faceting and abnormal grain growth in BaTiO₃. Acta Mater, 48:1575-80
- 118. Roberts CG. 2007. Grain growth and the Zener pinning phenomenon: a computational and experimental investigation. PhD thesis, Carnegie Mellon Univ., Pittsburgh, PA
- 119. Holm EA, Miodownik MA, Rollett AD. 2003. On abnormal subgrain growth and the origin of recrystallization nuclei. Acta Mater. 51:2701-16
- 120. Humphreys FJ. 1997. A unified theory of recovery, recrystallization and grain growth, based on the stability and growth of cellular microstructures—I. The basic model. Acta Mater. 45:4231-40



- 121. DeCost BL, Holm EA. 2017. Phenomenology of abnormal grain growth in systems with nonuniform grain boundary mobility. Metall. Mater. Trans. A 48:2771-80
- 122. Holm EA, Miodownik MA, Healey KJ. 2004. A subgrain growth model for strain-free grain nucleation during recrystallization. Mater. Sci. Forum 467-70:611-16
- 123. Liu Y, Militzer M, Perez M. 2019. Phase field modelling of abnormal grain growth. Materials 12:4048
- 124. Rudnizki J, Zeislmair B, Prahl U, Bleck W. 2010. Prediction of abnormal grain growth during high temperature treatment. Comput. Mater. Sci. 49:209-16
- 125. Kinoshita T, Ohno M. 2020. Phase-field simulation of abnormal grain growth during carburization in Nb-added steel. Comput. Mater. Sci. 177:109558
- 126. Fjeldberg E, Holm EA, Rollett AD, Marthinsen K. 2012. Mobility driven abnormal grain growth in the presence of particles. Mater. Sci. Forum 715-16:930-35
- 127. Messina R, Soucail M, Kubin L. 2001. Monte Carlo simulation of abnormal grain growth in two dimensions. Mater. Sci. Eng. A 308:258-67
- 128. Holm EA, Hoffmann TD, Rollett AD, Roberts CG. 2015. Particle-assisted abnormal grain growth. IOP Conf. Ser. Mater. Sci. Eng. 89:012005
- 129. Lee DK, Ko KJ, Lee BJ, Hwang NM. 2008. Monte Carlo simulations of abnormal grain growth by sub-boundary-enhanced solid-state wetting. Scr. Mater. 58:683-86
- 130. Frazier WE, Rohrer GS, Rollett AD. 2015. Abnormal grain growth in the Potts model incorporating grain boundary complexion transitions that increase the mobility of individual boundaries. Acta Mater. 96:390-98
- 131. Prajapati N, Späth M, Knecht L, Selzer M, Nestler B. 2021. Quantitative phase-field modeling of faceted crystal dissolution processes. Cryst. Growth Des. 21:3266-79
- 132. Chen J, Guo M, Yang M, Su H, Liu L, Zhang J. 2021. Phase-field simulation of γ' coarsening behavior in cobalt-based superalloy. Comput. Mater. Sci. 191:110358
- 133. Hwang NM, Lee SB, Kim DY. 2001. Abnormal grain growth by solid-state wetting along grain boundary or triple junction. Scr. Mater. 44:1153-60
- 134. Mason JK, Lazar EA, MacPherson RD, Srolovitz DJ. 2015. Geometric and topological properties of the canonical grain-growth microstructure. Phys. Rev. E 92:063308
- 135. Braun C, Dake JM, Krill CE, Birringer R. 2018. Abnormal grain growth mediated by fractal boundary migration at the nanoscale. Sci. Rep. 8:1592
- 136. Zeller RA, Fey HJ, Braun C, Birringer R, Krill CE III. 2019. Influence of rapid annealing on the evolution of fractal abnormal grains in nanocrystalline Pd-10 at% Au. IOP Conf. Ser. Mater. Sci. Eng. 580:012055
- 137. Koo JB, Yoon DY, Henry MF. 2000. Island grains of low misorientation angles formed during abnormal grain growth in Cu. Metall. Mater. Trans. A 31:1489-91
- 138. Bennett TA, Kalu PN, Rollett AD. 2007. On the character of host-island grain interfaces in Fe-1%Si alloy. Scr. Mater. 57:41-44
- 139. Hutchinson WB. 2012. Origin of Goss texture during secondary recrystallisation in silicon-steel. Mater. Sci. Forum 715-716:73-80
- 140. Rajmohan N, Szpunar JA. 2000. Monte-Carlo simulation of Goss texture development in silicon steel in the presence of MnS particles. Mater. Sci. Eng. A 289:99-108
- 141. Chen K, Han J, Pan X, Srolovitz DJ. 2020. The grain boundary mobility tensor. PNAS 117:4533-38

